JOURNAL OF ENGINEERING, SCIENCE & EDUCATION

Vol1 | No1 | 2024

The Editorial Board

Disclaimer

Neither the Journal editors nor the publisher (NITTTR Kolkata) warrants that contents in the articles are accurate or complete, we are not responsible for any errors or omissions or mistakes etc. Author(s) of each article of this Journal is/are solely responsible for the data presented herein are correct or sufficient to support the conclusion or that the experimental design or methodology is adequate.

Journal of Engineering, Science & Education

Published by
National Institute of Technical Teachers' Training and Research, Kolkata
(Ministry of Education, Government of India)
Block-FC, Sector-III, Salt Lake City, Kolkata-700106

Editorial

Namaskar. Inaugural issue of the Journal of Engineering Science & Education (JESE) has been published on 11th January 2024, the 60th Foundation Day of the Institute. The objective of JESE is to provide academic and industry with a platform for publication of research papers, review papers and communication letters allowing dissemination of knowledge in basic science, all discipline of engineering, pedagogy, education technology, patent review and ancient Indian science & technology. In this issue, results of scientific and experimental in the fields of material science, image processing and ensemble learning are included. Further, couple of articles in the field of Indian knowledge systems are presented in this inaugural issue of this journal.

All papers submitted to the JESE gone through per-reviewed process. Moreover, all aspects of submission, resubmission and notifications have been handled electronically. We are grateful to all authors for contribution of their works and reviewers for their efficient in valuable assistance in the formation of this issue of the "Journal of Engineering Science & Education". A special thanks given to Shri. Utpal Chakraborty, NITTTR Kolkata for compiling articles in a book form for this issue.

On behalf of all our editorial team and contributors, as the Editor-in-Chief of JESE wishing a great pleasure to publish this journal for academic interest and wish you all fruitful reading. Constructive suggestions and feedback from our readers are solicited for improving the overall quality of this journal.

Prof. Debi Prasad Mishra
Editor-in-Chief
Journal of Engineering, Science & Education

Exploring Kidney Cancer using Transcriptomic Data

Indrajit Saha[a,c,*], **Nimisha Ghosh**[b,c], **Somnath Rakshit**[a,c]

[a]*Department of Computer Science and Engineering, National Institute of Technical Teachers' Training and Research, Kolkata, West Bengal, India*

[b]*Department of Computer Science and Information Technology, Institute of Technical Education and Research, Siksha 'O' Anusandhan (Deemed to be University), Bhubaneswar, Odisha, India*

[c]*Equally contributed*

*Corresponding author, email: indrajit@nitttrkol.ac.in

Abstract

Kidney renal clear cell carcinoma is a common malignancy of kidney and has the highest mortality rate in all genitourinary cancers. Regardless of the advancement in medical science and cancer research, the incidents and mortality of this disease have risen in the last two decades. The delayed detection is one of the major causes behind this cancer. The identification of molecular biomarkers using omics technology can help in better prognosis and treatment of kidney cancer. Due to the recent advancements of Next Generation Sequencing techniques, the availability of high-throughput RNA-Seq data gives a new dimension in cancer studies. This fact motivated us to find not only the potential miRNA as biomarker for kidney cancer but also to find the association between miRNAs and their target mRNAs. In this regard, ensemble of decision trees is used in a systematic way to perform the classification and regression tasks separately for ranking of miRNAs and finding their association with mRNAs. The classification task is performed using AdaBoost integrated ensemble of decision trees in order to rank the miRNAs while regression analysis is performed using LSBoost integrated ensemble of decision trees to find their association with target mRNAs. Here survival of the kidney cancer patients as alive or dead is used as class label of the expression data of miRNAs to perform the classification task. The results of top ten miRNAs along with their top ten targets are considered for biological insight. In this regard, expression analysis of miRNAs and mRNAs using t-test along with miRNA-Gene-TF and PPI networks are analysed. Moreover, KEGG pathway and GO enrichment analysis have been conducted, which show significant cancer pathways including Renal Cell Carcinoma for the selected miRNAs and some important pathways involved in cancer development. The datasets, code and supplementary materials of this work are provided online[1].

Keywords: Ensemble learning; Kidney cancer; miRNA; mRNA; Next generation sequencing

[1] http://www.nitttrkol.ac.in/indrajit/projects/mirna-mrna-kidneycancer/

1. Introduction

Kidney renal clear cell carcinoma (KIRC) is the most common kidney cancer having high mortality all over the world[2]. In addition to often arising as globular masses that occasionally protrude beyond the usual contour of the kidney, KIRC can originate anywhere in the renal cortex. They can, however, occasionally infiltrate widely or grow inward. Usually consisting of soft bright yellow parenchyma with patches of grayish edematous stroma, haemorrhage, necrosis, and cysts, the cut surface is varied. The cysts are filled with either haemorrhage or a clear, straw-colored fluid [1]. It has become a widespread malignancy in the last two decades. The reason behind this is mainly poor prognosis and late detection. KIRC, if not metastasized, is curable by surgery. This suggests the necessity of looking at this problem from clinical and computational perspectives and to identify biomarkers related to this cancertype. Some recent studies have proposed that miRNAs can act as potential biomarkers for KIRC [2].

MicroRNAs (miRNAs) are small (19-22 nucleotide long) and non-coding RNAs that negatively control the gene expression. miRNAs bind with the complementary sequences of the target mRNAs in 3'- untranslated region (UTR) or even in other regions of those mRNAs and result in RNA splicing. It is evidenced that miRNAs are involved in various cellular functions such as development of cells, cell differentiation and metabolism [3]. It has been experimentally found that due to both tumor suppression and oncogenesis nature of miRNAs, they show divergent expression patternsand mutation in various cancer types. The selection of proper miRNAs is, therefore, important to provide a better prognosis and treatment of KIRC. In this regard, nowadays high-throughput sequencing is the primary choice to measure expression levels, i.e., RNA-Seq. In such cases, no prior knowledge of the reference or sequence of interest is needed. It also enables for a wide range of applications [4]. RNA- Seq technology has been widely used for identification of biomarkers in KIRC. Moreover, for understanding the underlying cause of disease it is always suggested to identify the causative biomarkers. As already described, miRNAsand mRNAs are two such important biomarkers involved in biological processes as well as diseases. Understanding their relation with respect to a disease may help in developing efficient diagnostic and prognostic tools. In this regard, Wotschofsky et al. [5] studied the role of miRNAs and mRNAs in KIRC. In [6], Khatibi et al. have used feature selection methods based on filter and graph algorithm to identify miRNAs and mRNAs for renal cell carcinoma subtypes which includes KIRC, KIRP and KICH. In this regard, the authors have identified 77 mRNAs and 73 miRNAs to differentiate among such subtypes with 92% and 95% accuracies respectively. Tensor decomposition (TD)-based unsupervised learning was used in [7] to analyse mRNA and miRNA expression profiles of KIRC genes. Their experimental results showed that out of all the genes related to cancer pathways, 23 were highly correlated with the survival of KIRC patients. However, finding the association between miRNAs and mRNAs by ranking them using statistical learning techniques is important to shortlist the miRNAs and their targets (mRNAs) for clinical trials.

To address the above fact, in the current work, Next Generation Sequencing (NGS) [8] provided miRNA and mRNA expression data with clinical detail, such as survival of patients of KIRC are used. The patients are classified into alive or dead based on their survival status in order to determine responsible miRNAs for KIRC. In this regard, AdaBoost integrated ensemble of decision trees [9] is used to classify and rank the features (miRNAs) for further analysis. The target mRNAs are identified for the top ranking miRNAs by performing regression analysis using LSBoost integrated decision trees [9]. Finally, their roles in various important biological

[2] https://www.cancer.org/cancer/kidney-cancer/detection-diagnosis-staging

functions and networks are demonstrated.

2. Materials and Method

2.1. Brief Description of Ensemble Learning

Adaboost is an ensemble classifier, whose output combines the result of multiple classifiers. It combines multiple weak classifiers to form a strong classifier. The short trees contain one decision for classification, these are called decision stumps. Adaboost can be thought as adaptive since the subsequent weak learners are tweaked to match the instances that were wrongly classified by previous learners. The final tree can be used to obtain the importance of the features (miRNAs) by getting the values of Gini index. On the other hand, regression analysis is a statistical tool to estimate the relation between variables. It helps in understanding how the dependent variable changes with a change in one or more of independent variables. Least square is a standard method used in regression analysis for approximating the solution of overdetermined systems. This idea is used in LSBoost integrated ensemble of decision trees algorithm. A prediction model is produced in a structure of an ensemble of weak prediction models, mostly decision trees. The model builds in a stepwise pattern and in each step, a new learner is fitted by ensemble by considering the difference between the actual response and aggregated prediction of all the learners considered earlier by allowing ensemble fits to optimize mean-squared error. Similarly, like previous case, Gini index values can be used to rank the features (miRNAs) using the final decision tree.

2.2. Data Preparation

The NGS provided high-throughput miRNA and mRNA expression data (in the form of RNA-Seq) with clinical information are collected from TCGA. The miRNA expression data contains 544 miRNAs and 17,942 mRNAs for 326 patients affected by KIRC whereas the clinical information contain age, status (alive/dead), days to follow-up and gender of the patients. The expression of the miRNA and mRNA is generated using Illumina high sequencing technique in the form of reads per million count and later normalized into log2 scale. miRNAs and mRNAs with more than 60% zeroes are discarded from both the expression datasets prior to the experiment. The statistics of the dataset is provided in Table 1.

Table 1: *Statistics of the dataset*

Status	No. of patients		Average Age	No. of days to last follow-up
	Male	Female		
Alive	152	72	58.17	1631.47
Dead	72	30	64.61	1053.75

2.3. Method

The flowchart of the work is shown in Figure 1. In this regard, AdaBoost and LSBoost integrated ensemble of decision trees are applied separately for classification and regression respectively. First, the AdaBoost integrated ensemble of decision trees is used to rank the miRNAs using Gini index value of the decision trees. For this purpose, the expression values of the miRNAs along with their class label as survival of the patients (alive/dead) are used. This gives a score associated with each miRNA in order to rank them. Thereafter, miRTarBase is used to find the target mRNAs with respect to these miRNAs. As a result, the mRNAs are obtained for each of the miRNA. Next, in order to find the association between miRNA and mRNAs, LSBoost integrated ensemble of decision trees is used to perform regression analysis. After the regression analysis, the target mRNAs are ranked based on their corresponding estimated value in terms of Gini index. Here, higher value indicates stronger association of the miRNA-mRNA pair that are involved in the survival of patient. Note that -log10 of such value is computed to report in the results section for readability where lower score indicates higher association. The validation of the pairs is shown in the last level of the flowchart. Finally, the pairs are validated using expression analysis, miRNA-Gene-TF network, PPI network, KEGG pathway and GO enrichment analysis.

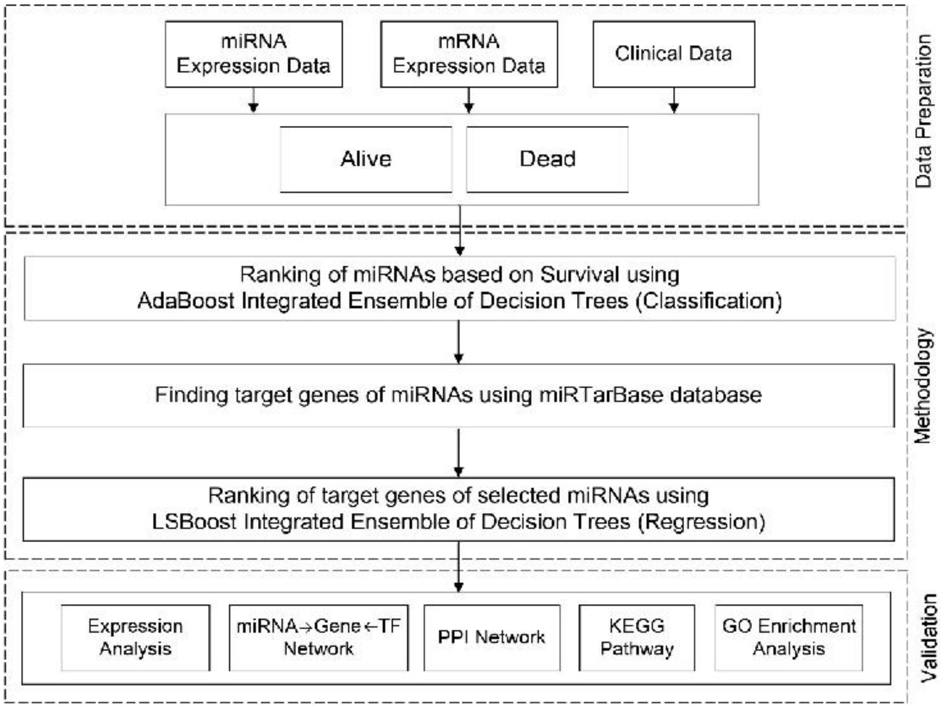

Figure 1: *Steps of the proposed method to rank the miRNA-mRNA pairs*

3. Results and Discussion

3.1. Experimental Testbed

The experiment is carried out by using MATLAB 2018a while Pandas 0.23 and Numpy 1.14 are used in Python 3.6.5 while for computation, an intel i7 processor with 8 GB RAM and 8 cores are used.

3.2. Results and Validation

AdaBoost integrated ensemble of decision trees is used for the classification in order to rank the miRNAs. As a result, some miRNAs are identified and ranked based on the value of -log10(Gini index) and named as 'Score'. From such list, top ten miRNAs, viz. hsa-miR-1291, hsa-miR-92a-3p, hsa-miR-187-3p, hsa-miR-3615, hsa-miR- 148a-5p, hsa-miR-149-5p, hsa-miR-939-5p, hsa-miR-590-3p, hsa-miR-937-3p and hsa-miR-130a-3p are considered for further study while the rest are provided in the supplementary. Thereafter, the target mRNAs of these ten miRNAs are identified using miRTarBase database. The expression value of these target mRNAs is used for the regression analysis and depending on the score, the mRNAs are ranked. Higher rank of the mRNAs signifies stronger association between miRNA and mRNA. Such results of miRNA-mRNA association are reported in Table 2 with the score and PubMed ID. Note that all the ten miRNAs have at least ten targets except hsa-miR-1291, hsa-miR-3615 and hsa-miR-590-3p which have eight, nine and seven targets respectively. Thus, 94 unique mRNAs are obtained to make pairs and their evidence is also found in literature. In order to visualize their change in expression based on survival status of the patients, expression analysis has been performed on the miRNA-mRNA pairs using boxplots as shown in Figure 2. Moreover, a two sample t-test has been performed on the expression of miRNA-mRNA pairs to see their statistical significance. As a result, it is found that hsa-miR-92a-3p and BCL2L11, hsa-miR-149-5p and BBC3, hsa-miR-187-3p and S100A4 and hsa-miR-590-3p and ITPRIPL1 are having significant association with p-values 7.06e-282, 5.69e-189, 1.82e-274 and 1.53e-125 respectively and reported in Figure 2 also.

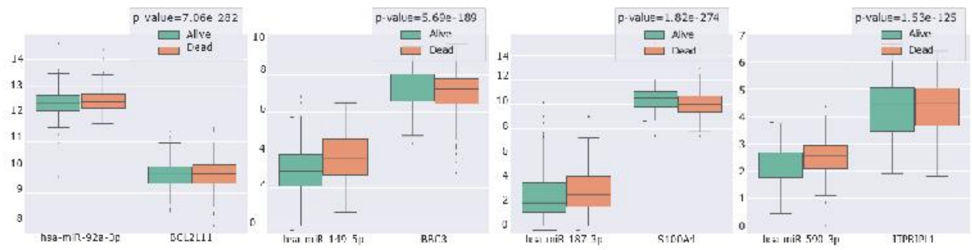

Figure 2: *Boxplot of the top miRNA-mRNA pairs in order to show the change in expression*

The top ten miRNAs and their 94 targets are used to identify the Transcription Factors (TFs) using TransmiR and TRRUST databases in order to prepare the miRNA-Gene-TF network. It is shown in Figure 3 (a), where orange, violet and blue colours represent miRNA, mRNA and TF respectively. The TFs that are associated with 94 mRNAs for the ten miRNAs are found using TransmiR database. Such TFs are used to prepare the PPI network using STRING database and shown in Figure 3 (b). A bar plot showing the degree of the top ten nodes is also shown in the same figure. It is seen that well known kidney cancer related TFs like MYC, ESR1, CREB1, IL6, etc. as found in literature [10,11, 12] are also seen in the PPI network as a node with higher degree. Thereafter, all the obtained mRNAs that are associated with top ten miRNAs are considered to identify their significance in KEGG pathways and Biological Process (Gene Ontology). In this regard, Enrichr Tool is used. Different cancer pathways are found which are shown in Figure 4 (a).

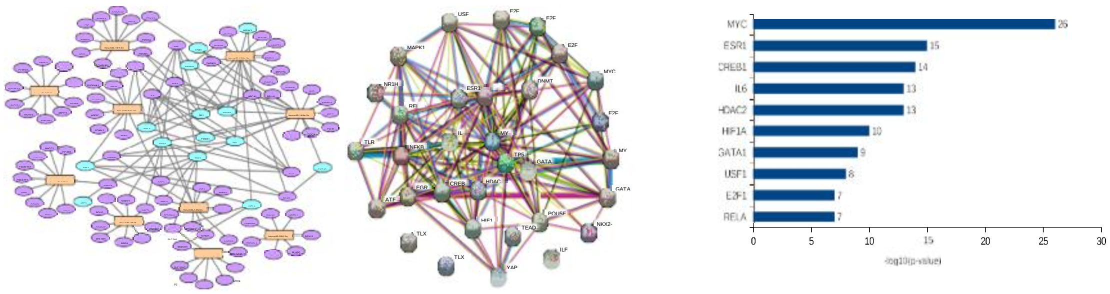

(a) (b)

Figure 3: *(a) miRNA-Gene-TF network by considering top ten miRNAs with their 94 targets, (b) PPI Network of the TFs that are associated with the mRNAs of the selected miRNAs and degree of the top ten nodes in the PPI Network are shown in bar*

Table 2: *Top ten miRNAs obtained through our approach and their target mRNAs*

miRNA	mRNA	Score	PubMed ID	miRNA	mRNA	Score	PubMed ID
	GTPBP2	3.945	21572407		FOXM1	2.945	23762558
	GOLGA8B	4.016	23446348		SERPINH1	3.515	21572407
	FAM83G	4.068	23592263		ZBTB2	3.579	23144691
	SLC12A7	4.079	22291592		BBC3	3.601	23873935
hsa-miR-1291	PFKFB3	4.148	23592263	hsa-miR-149-5p	MTHFR	3.610	28045918
	HIST1H4H	4.155	23446348		PTGER2	3.618	25916550
	GOLGA8A	4.185	23592263		IL6	3.667	25916550
	SLC2A1	4.229	23889809		MYD88	3.696	24375488
	-	-	-		GIT1	3.744	24608434
	-	-	-		NONO	3.801	23622248
	FGF2	4.105	23622248		UNC13A	4.292	23592263
	PTEN	4.149	24026406		QSOX2	4.319	23592263
	BCL2L11	4.179	21883694		CLSTN1	4.412	23592263
	H3F3C	4.288	23592263		SYNGR1	4.459	23592263
hsa-miR-92a-3p	DUSP5	4.341	22473208	hsa-miR-939-5p	MSN	4.530	20371350
	DNAJB9	4.341	22473208		ABCC5	4.564	26701625
	TMF1	4.377	23622248		SLC34A2	4.565	28114937
	PLEKHA1	4.392	23592263		ICOSLG	4.619	20371350
	FOXN2	4.485	22473208		SEPT8	4.633	22012620
	SOX4	4.542	22473208		ABCF2	4.708	24398324
	BCL6	2.497	26845350		PLA2G7	3.467	23824327
	CRMP1	3.083	27864146		EIF4A2	3.887	23446348
	DYRK2	3.152	22012620		ITPRIPL1	3.946	23446348
	CCDC115	3.203	23446348		PEX13	3.988	22012620
hsa-miR-187-3p	LZIC	3.274	23592263	has-miR-590-3p	MBTD1	3.992	21572407
	CCNB1IP1	3.277	23446348		BANK1	4.025	20371350
	S100A4	3.424	27544906		HNRNPF	4.081	26701625
	MRO	3.486	21572407		-	-	-
	CENPA	3.516	23446348		-	-	-
	FOXA2	3.614	28098868		-	-	-
	POLQ	3.439	23824327		DCAF8	4.063	23622248
	RPS8	3.889	23622248		CAMK2N2	4.099	19536157
	ACSM2A	3.946	24906430		GDF15	4.238	26701625
	TAB1	3.979	23824327		GLUL	4.240	23622248
hsa-miR-3615	PDLIM3	4.023	23824327		MON1B	4.299	27418678
	SPRY1	4.034	23622248		CBFA2T3	4.317	23313552
	ZNF682	4.052	23824327		CPOX	4.369	23622248
	CD300E	4.070	24906430		FOXQ1	4.490	23592263
	WNT4	4.141	23824327		NACC1	4.578	26701625
	-	-	-		PEX6	4.817	23592263
	CALR	3.602	23446348		RUNX3	3.693	22846564
	CDCA4	3.665	24398324		RPS27A	3.771	23592263
	SH3GLB1	3.869	22100165		MMGT1	3.809	23592263
	ABCA1	3.891	26437365		ZNF12	3.869	24398324
hsa-miR-148a-5p	KHSRP	3.922	23446348	has-miR-130a-3p	BLCAP	3.956	23592263
	ATP5G3	3.926	23592263		PPARG	3.983	21135128
	APC2	3.962	23592263		BTBD3	3.993	23592263
	MX2	4.034	23824327		SMAD4	4.037	23418453
	RPL41	4.089	20371350		TNF	4.104	24885472
	AKT2	4.187	27878305		ZNF800	4.140	23592263

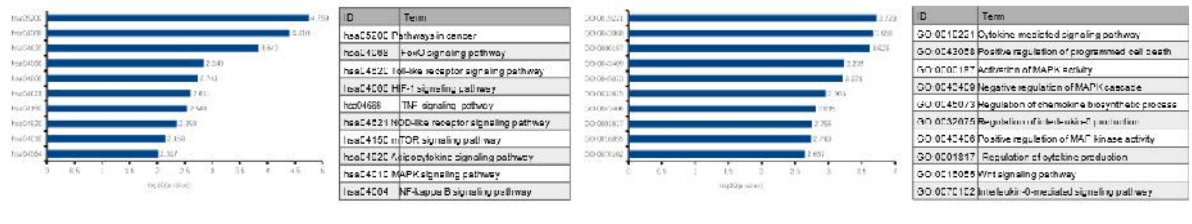

(a) (b)

Figure 4: *Bar plot of the significant (a) KEGG pathways and (b) GO Enrichment Biological Process terms based on -log10(p-value)*

This analysis signifies that these mRNAs actively play a significant role in KIRC by affecting pathways like Pathways in cancer, FoxO signaling pathway, Toll-like receptor signaling pathway, HIF-1 signaling pathway and TNF signaling pathway. Moreover, the Gene Ontology terms for Biological Process are also obtained. This is shown in Figure 4 (b). Some important terms are reported like Cytokine-mediated signaling pathway, Positive regulation of programmed cell death, Activation of MAPK activity, Negative regulation of MAPK cascade, Regulation of chemokine biosynthetic process, Regulation of interleukin-6 production, Positive regulation of MAP kinase activity, Regulation of cytokine production, Wnt signaling pathway and Interleukin-6-mediated signaling pathway. Therefore, the findings suggest that selected miRNA-mRNAs pairs are statistically and biologically relevant in etiology of kidney cancer.

4. Conclusion

In the current work, miRNAs with significant role in KIRC have been identified and they have been ranked based on patient status using AdaBoost. Also, the target mRNAs of these miRNAs have been identified and ranked through LSBoost by performing regression analysis. The obtained pairs show ample evidence in the existing literature regarding their dominant role in KIRC. Moreover, during the biological analysis, these mRNAs are found to be present in KIRC pathways which shows the importance of the selected miRNA-mRNA pairs in KIRC. As a scope of further research, similar study can be conducted to rank and select important miRNA-mRNA pairs in other cancer types.

References

1. J. N. Eble, L. Cheng, Chapter 30 - renal neoplasia, in: Modern Surgical Pathology (Second Edition), second edition Edition, W.B. Saunders, Philadelphia, 2009, pp. 1043–1078.
2. W. M. Linehan, R. Srinivasan, L. S. Schmidt, The genetic basis of kidney cancer: a metabolic disease, Nature Reviews Urology 7 (5) (2010) 277–285.
3. M. A. Valencia-Sanchez, J. Liu, G. J. Hannon, R. Parker, Control of translation and mrna degradation by mirnas and sirnas, Genes & Development 20 (5) (2006) 515–524.
4. J. Costa-Silva, D. Domingues, F. M. Lopes, Rna-seq differential expression analysis: An extended review and a software tool, PLOS One 12 (12) (2017) e0190152.
5. Z. Wotschofsky, L. Gummlich, J. Liep, C. Stephan, E. Kilic, K. Jung, J.-N. Billaud, H.-A. Meyer, Integrated microrna and mrna signature associated with the transition from the locally confined to the metastasized clear cell renal cell carcinoma exemplified by mir-146-5p, PLOS One 11 (2) (2016) e0148746.
6. S.M.K Hosseiniyan, M. Ardalan, M. Teshnehlab, Panels of mRNAs and miRNAs for decoding molecular mechanisms of Renal Cell Carcinoma (RCC) subtypes utilizing Artificial Intelligence approaches, Scientific Reports, 12 (2022), 16393.
7. K-L. Ng, Y.-H. Taguchi, Identification of miRNA signatures for kidney renal clear cell carcinoma using the tensor-decomposition method, Scientific Reports, 10, (2020),15149
8. S. Goodwin, J. D. McPherson, W. R. McCombie, Coming of age: ten years of next-generation sequencing technologies, Nature Reviews Genetics 17 (6) (2016) 333–351.
9. J. Friedman, T. Hastie, R. Tibshirani, The elements of statistical learning, Springer, 2001.
10. E. H. Shroff, L. S. Eberlin, V. M. Dang, A. M. Gouw, M. Gabay, S. J. Adam, D. I. Bellovin, P. T. Tran, W. M. Philbrick, A. Garcia-Ocana, et al., MYC oncogene overexpression drives renal cell carcinoma in a mouse model through glutamine metabolism, Proceedings of the National Academy of Sciences 112 (21) (2015) 6539–6544.
11. T. Yao, Q. Wang, W. Zhang, A. Bian, J. Zhang, Identification of genes associated with

renal cell carcinoma using gene expression profiling analysis, Oncology letters 12 (1) (2016) 73–78.

12. Z. Fang, A. Lin, J. Chen, X. Zhang, H. Liu, H. Li, Y. Hu, X. Zhang, J. Zhang, L. Qiu, et al., Creb1 directly activates the transcription of ribonucleotide reductase small subunit m2 and promotes the aggressiveness of human colorectal cancer, Oncotarget 7 (47) (2016) 78055– 7806.

Optimization of density and hardness of graphite-copper composites by using Taguchi method

Jhulan Kumar and Subrata Mondal*
Department of Mechanical Engineering
National Institute of Technical Teachers' Teacher Training and Research, Kolkata,, West Bengal, India

* *Corresponding author, email: subratamondal@nitttrkol.ac.in*

Abstract

Copper is extensively used for various industrial applications due its high electrical and thermal conductivity, however, poor mechanical properties hindered its applications. As a reinforcement material, graphite reduces weight of composite at the same time enhances the mechanical property of the composites for advanced material applications. This paper presents optimization of hardness and density of graphite-copper composites by using Taguchi's optimization methodology. Analysis of variance is used to study the influence of compaction pressure, reinforcement concentration and sintering temperature on hardness and sintered density of composite materials. Measured data were analysed with the help of MINITAB15 software. Signal –to – noise ratio was used to analysed effect of reinforcement concentration, compaction pressure and sintering temperature on sintered density and hardness properties. Results indicates that reinforcement concentration in the composite is the most notable parameter on sintered density, while, sintering temperature has the most significant influence on hardness properties of composite.

Keywords: Composite materials; hardness; optimization; powder metallurgy; sintered density.

1. Introduction

Composites materials are artificially produced multiphase materials. These materials are produced in order to utilize the advantages of various properties of bulk material such as metal (or metal alloy) or ceramics (or ceramic alloy) or polymers (or polymer blend) and minor portion of organic materials (e.g. Kevlar, cellulosic fibers etc.) or inorganic materials (e.g. silicon carbide, various carbon material, boron etc.) in a tailor made material. The composites materials are manufactured from at least two materials in such a manner that individual components retain their identity while bonded together in the resultant material. The constituent materials are not soluble in each other and no other chemical reaction takes place. The major portion material is called as matrix domain while minor portion is the reinforcement. The strength of the composite is generally in between matrix and reinforced material in case of proper distribution and dispersion of reinforcement material in the matrix phase with good bonding between the various phases.

Matrix phase bonds reinforcements and helps to transfers load from one phase to another phase and vice versa. In general matrix is soft in nature as compared with the reinforcement phase. On the other hand, reinforcing phase improves mechanical and other physical properties of resultant composite materials. Generally, reinforcement is harder, stronger and stiffer than matrix [1, 2]. The geometry of the reinforcement particles is one of the major parameters for determining the performance of the composite materials. Properties of composites materials depends on the shape, size, and dimensions of the reinforcement particles. The reinforcing phases could be fibers, particles, flakes types etc. and size could be macro, micro, nano etc. Composite materials prepared with particle like reinforcements has almost equal dimension in all directions. The shape of the reinforcing particles may be spherical, cubical, cylindrical, plate like and may have regular or irregular geometry.

Metal matrox composite, polymer matrix composite and ceramic matrix composites are various classifications of composite materials based on the matrix phase. In MMC, Al, Cu, Mg, Ti etc. are more commonly used as matrix phase. These composites can operate at high temperature as compared to the PMC. Metal matrix composites have several conveniences over the pure metals such as better specific strength, lighter, higher modulus, improved properties at elevated temperatures, improved wear resistance properties and lower coefficients of thermal expansion. However, their toughness is inferior to monolithic metals. Copper is widely used for many industrial applications such as heating element, motor vehicle radiator, air conditioner, electrical generator, electronic goods etc. Some of the drawback of copper are high cost, soft and ductile etc. and these drawbacks could be improved by reinforcing appropriate reinforcing phase in the matrix domain.

Yang et al. presents copper-carbon composite fabricated by using molding and sintering method. Bonding between carbon particles and matrix domain has been improved by the incorporation of pitch coke. Excellent interfacial bonding between reinforcements and matrix phases enhances the strength of the copper composite material. The micro-hardness of composites has been improved with increase in the content of pitch coke [3]. Power presents copper-carbon composite prepared by using powder metallurgy in different weight fraction of reinforcement material. The hardness of copper-graphite composite decreases with the weight percentage of graphite particulates [4]. Graphite reinforced copper matrix composites preparation by employing casting process has been reported in Ref [5]. The hardness of the prepared composite samples increases with the concentration of graphite. Microstructure study exhibits presence of copper and along with some copper oxide formation. Detailed microstructure analysis revealed excellent interfacial interaction between copper matrix and graphite reinforcement. Density of the composite materials has been increased with increase in the content of graphite by weight due to the formation of more compact structure.

Hardness property of copper (Cu) matrix composite material is an important parameter which may influence other properties *viz.* wear, compressive strength etc. of the resultant composite materials. Therefore, there is need for the optimization of process parameters for to obtain possible highest hardness and lowest density response. The Taguchi method design with three process parameters such as graphite (Gr) concentration, compaction pressure and sintering temperature are studied in the current paper to optimize Gr-Cu composite's sintered density and hardness behaviour. In order to maximize sintered density and hardness property, the experimental results are analysed to reveal the best possible process parameters combinations.

2. Experimental

2.1 Materials

Copper based metal matrix composites have unique properties and it is used widely in the manufacturing industries. Copper exhibits good ductility, electrical conductivity and thermal conductivity properties. While, graphite possesses excellent physical and mechanical properties. Therefore, copper has been selected as the matrix domain and graphite as a reinforcement domain to fabricate the composite materials. Properties of raw materials are described elsewhere [6].

2.2 Fabrication of Composites

Graphite reinforced composite materials are fabricated by using powder metallurgy route. Whole process has been depicted schematically in Figure 1. The detail fabrication process has been described elsewhere [6]. Copper matrix was reinforced with three different concentration of graphite, such as 5, 10 and 15 wt/wt%. Samples were compacted by universal testing machine (UTM) at three compaction pressure *viz.* 509.29, 572.55 and 636.61 MPa. Compacted samples were sintered at three different temperature, such as 900, 950 and 1000 °C.

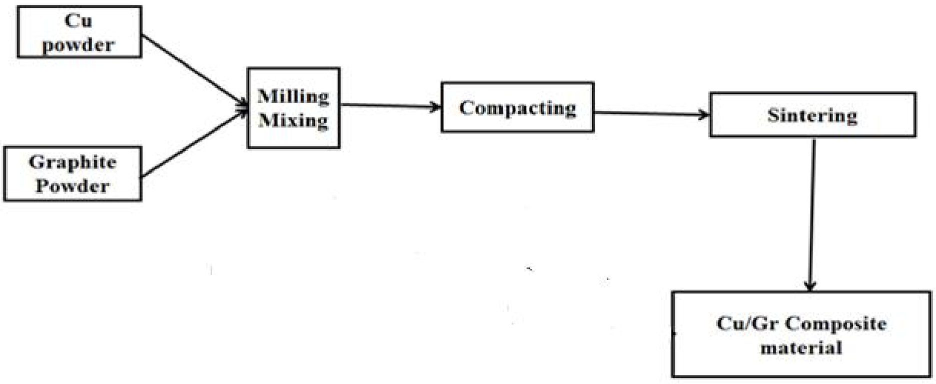

Figure 1: *Schematic representation of the copper graphite composite fabrication process*

2.3 Measurement of Density and Hardness

Sintered density of composite samples were measured by gravimetric method. The parameters required to measure the density are diameter (d) and length (l) of specimens that have been measured three times in each samples by digital Vernier calliper, and mass of each samples has been measured by digital weighing machine. Hardness is the property of a material to resists permanent indentation. Hardness measurement for each sample has been done in a Rockwell hardness tester. Detailed process for the measurement of sintered density and hardness are described elsewehre [6].

2.4 Optimization using Taguchi method

This method is used for the experimental design and analysis of experiments. The method runs are organized as per design of experiments based on the orthogonal arrays. In orthogonal arrays, the number of experiments runs is reduced and every process parameter is analyzed by keeping other parameter as constant. Influence of other parameters and significant parameters are decided on the basis of statistical analysis of the experimental response. Signal to Noise ratio (S/N) can be used to analyze the experimental data, which could be helpful for the designers. S/N ratio is a log function and this is used to calculate the deviation between the desired value and experimental value. This function can give the optimum value. The optimal setting is the process parameter combination, which gives the highest S/N ratio. The selection of appropriate orthogonal array depends on the degree of freedom of the variables. The three level variables have two degrees of freedom. The combination of the design of experiment with the optimization of control parameters to get the best result is achieved in the Taguchi methods. Table 1 shows the L-9 orthogonal array way of solving the problem in Taguchi method.

The optimization of experimental design is performed using Taguchi method and used to create a set of newly designed experiments by MINITAB software17. In this design Taguchi L9 (3*3) Orthogonal Array is designed to calculate S/N ratio, where the factor is 3 and number of experiment runs are 9.

Table 1: *L9 orthogonal array with design factors*

Sample No.	Concentration of graphite (wt/wt%)	Sintering Temperature (°C)	Compaction Pressure (MPa)
1.	5	900	509.29
2.	5	950	572.55
3.	5	1000	636.61
4.	10	900	572.55
5.	10	950	636.61
6.	10	1000	509.29
7.	15	900	636.61
8.	15	950	509.29
9.	15	1000	572.55

As per the Taguchi's method, the S/N ratio is calculated as the lower the better (LB) and the higher the better (HB). Relevant equation is as follows:

$$HB: \eta = -10 \log\left[\left(\frac{1}{n}\right) \sum_{i=1}^{n} \frac{1}{y2} \right]$$

$$LB: \eta = -10 \log\left[\left(\frac{1}{n}\right) \sum_{i=1}^{n} y^2 \right]$$

In this optimization process, the main aim is to maximize hardness and density. Therefore, the larger is the better type signal to noise ratio is applied to get the best result for sintering process.

$$HB: \eta = -10 \log\left[\left(\frac{1}{n}\right) \sum_{i=1}^{n} \frac{1}{y2} \right]$$

where, η= S/N ratio

n= number of repetition of experiment

y= observed response value

η represents the achieved S/N ratio calculated from observation table. n denotes the total no of experiments, **y** denotes the value of response for i^{th} number of the experiment.

From the experimental finding all the observation such as sintered density and hardness can be obtained, afterwards, S/N ratios are calculated. Different graphs for analysis is drawn by using MINITAB software (version-17). Process parameter combinations can be predicted by using S/N ratio and ANOVA.

3. Results and Discussion

3.1 Main effect plots for sintered density

Sintered densities of composites with different concentration of graphite is tabulated in Table 2. Sintered density of different graphite containing specimens compacted at 636.61 MPa pressure, and sintered at three different temperature are reported in our earlier publication [6]. Experimental results revealed that density of the composite could be lowered by increasing the graphite contents due to the lower density of graphite in comparison with the copper. Moreover, if the quantity of graphite was reinforced in composite too much, the graphite cluster could be formed, and organization of graphite agglomeration is also one of the factors leading to lower the density of resultant composite materials. The measured densities are always much lower than the theoretical densities. The porosity of composites increases by increasing graphite content and this may affect other properties of composites such as hardness, and other mechanical properties of materials.

The effect plots in Figure 2 indicate that the sintered density is significantly influenced by composition, sintering temperature and compaction pressure. This graph indicates that as the compaction pressure and sintering temperature increases, the sintered density also increases. However, the effect of composition is most significant compared to sintering temperature and compaction pressure on the sintered density of the samples. The changes in sintered density is more when weight percentage of graphite is increases. Therefore, the composition of composites strongly affects the sintered density. Vairamuthu et al. reported that the sintering temperature and compaction pressure strongly influence density of the aluminium matrix composites reinforced with ceramic nanoparticles [7]. Figure 3 presents the residual plot for S/N ration of sintered density, the relevant data are tabulated in Table 2. Table 3 shows the analysis of variation data.

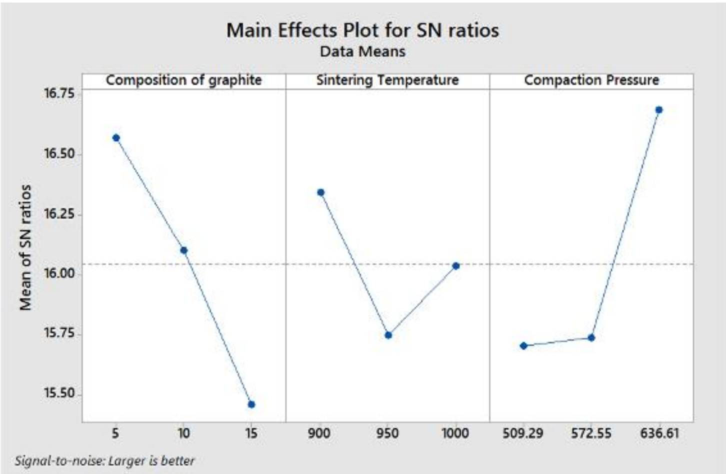

Figure 2: *Main effects plots for S/N ratio of sintered density.*

Table 2: *Experimental result and corresponding S/N ratio for sintered density.*

Composition (wt.% of graphite)	Compaction Pressure (MPa)	Sintering Temperature (°C)	Sintered Density (g/cc)	S/N Ratio
5	509.29	900	6.478	16.2288
5	572.55	950	6.576	16.3592
5	636.61	1000	7.184	17.1273
10	572.55	900	6.324	16.0198
10	636.61	950	6.415	16.1439
10	509.29	1000	6.412	16.1399
15	636.61	900	6.910	16.7896
15	509.29	950	5.462	14.7470
15	572.55	1000	5.521	14.8404

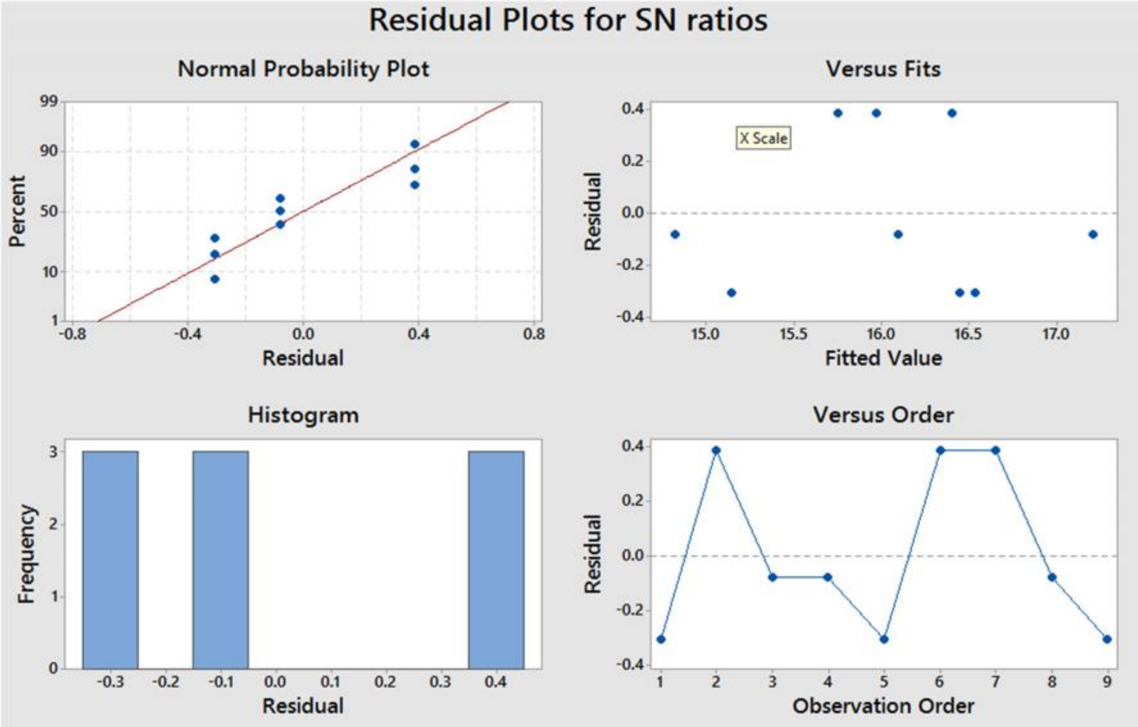

Figure 3: Residual plots for S/N ratio of sintered density.

Table 3: *Analysis of variance for means (density)*

Analysis of Variance for SN ratios

Source	DF	Seq SS	Adj SS	Adj MS	F	P
Composition of graphite	2	1.8723	1.8723	0.9361	2.51	0.285
Sintering Temperature	2	0.5331	0.5331	0.2666	0.71	0.583
Compaction Pressure	2	1.8620	1.8620	0.9310	2.50	0.286
Residual Error	2	0.7463	0.7463	0.3731		
Total	8	5.0136				

S = 0.6108   R-Sq = 85.1%   R-Sq(adj) = 40.5%

3.2 Main effect plots for average hardness

Hardness of composites with different concentration of graphite is tabulated in Table 4. Sintered density of different graphite containing specimens compacted at 636.61 MPa pressure, and sintered at three different temperatures are reported in our earlier publication [6]. Denser samples will have higher hardness values. Composite materials sintered at 900 and 1000 °C, the hardness of copper-graphite composites has been improved with increasing graphite concentration up to certain graphite concentration. Increase of graphite weight concentration up to 10%, hardness of composite materials increases, afterwards, decreases with reinforcement concertation. Maximum hardness value reported about 35 percent increase over that of the pure copper. The hardness of composite with higher graphite concentration decreases due to the clustering of graphite and formation of porosity in the composite materials. The hardness of composite materials depends on concentration of graphite together with porosity of the materials. Composite with higher density has improved hardness property as compared with less denser material. Optimization of processing parameters is very important to tailor the properties of composite materials [8].

The effect plots in Figure 4 indicates that the hardness is significantly influenced by sintering temperature and compaction pressure. Further, the hardness is more affected by composition. These graphs indicates that as the sintering temperature and compaction pressure increase, hardness is also increases. It is clearly observed that the composition of graphite strongly affects average hardness, and the maximum hardness is found at 10 % wt. graphite. Earlier research reported that the compaction pressure and sintering temperature strongly influence hardness of the ceramic particles reinforced aluminium matrix composites [7]. In another paper in earlier research, it has been reported that higher compaction pressure, sintering temperature and reinforcement weight percentage were resolved as suitable parameters to obtain maximum hardness [9]. Research by Srinivas et al. revealed that Taguchi optimization of mechanical characteristics of composite materials fabricated by powder metallurgy are highly relied upon the sintering temperature and slightly on sintering time and compacting pressure [10].

Figure 5 presents residual S/N ratio of hardness, the relevant data are presented in Table 4 and the analysis of variation of hardness data are tabulated in Table 5.

Table 4: *Experimental result and corresponding S/N Ratio for average hardness.*

Composition (wt.% of graphite)	Sintering Temperature (°C)	Compaction Pressure (MPa)	Average Hardness (Rockwell)	S/N Ratio
5	509.29	900	64	36.1236
5	572.55	950	68	36.6502
5	636.61	1000	88	38.8897
10	572.55	900	75	37.5012
10	636.61	950	74	37.3846
10	509.29	1000	88	38.8897
15	636.61	900	53	34.4855
15	509.29	950	61	35.7066
15	572.55	1000	76	37.6163

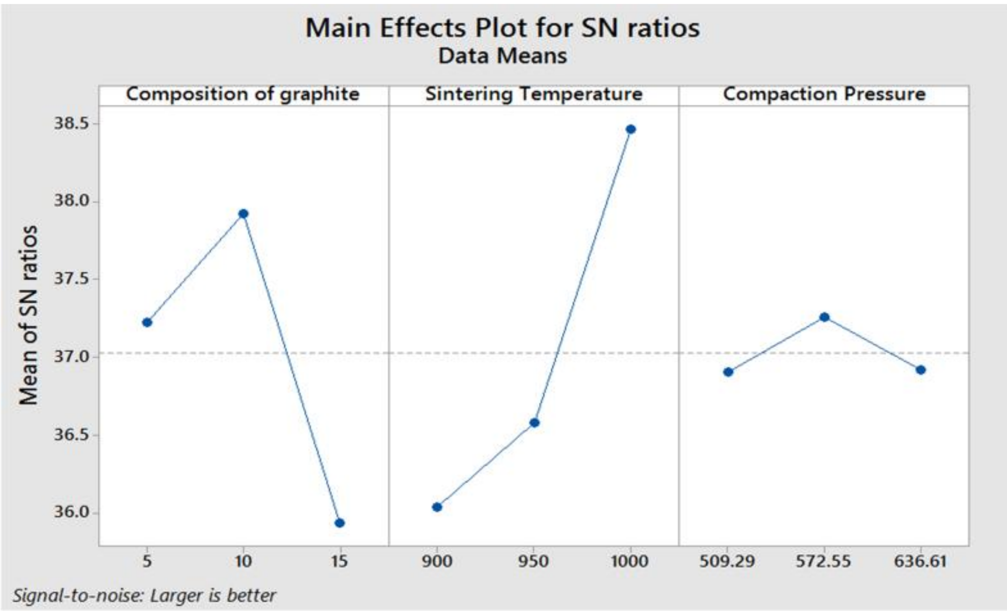

Figure 4: *Main effects plots for S/N ratio of average hardness (Rockwell)*

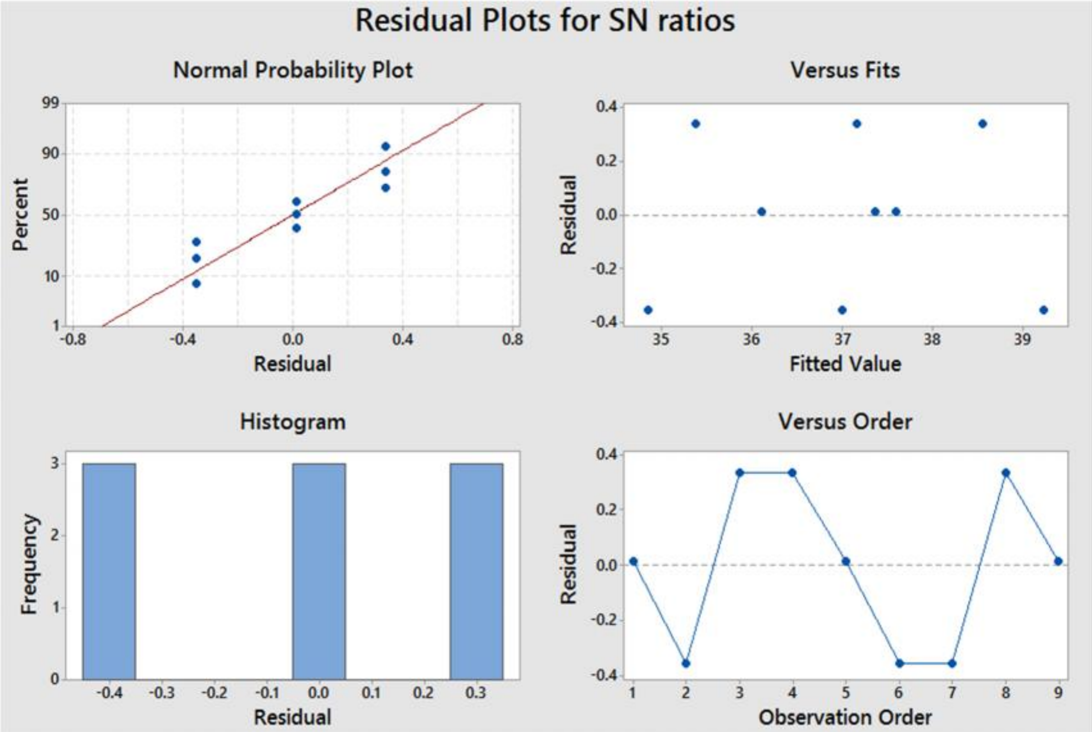

Figure 5: *Residual plots for S/N ratio of hardness (Rockwell).*

Table 5: *Analysis of variance for means (hardness)*

Analysis of Variance for Means

Source	DF	Seq SS	Adj SS	Adj MS	F	P
Composition of graphite	2	377.56	377.556	188.778	9.71	0.093
Sintering Temperature	2	680.22	680.222	340.111	17.49	0.054
Compaction Pressure	2	6.22	6.222	3.111	0.16	0.862
Residual Error	2	38.89	38.889	19.444		
Total	8	1102.89				

S = 4.410   R-Sq = 96.5%   R-Sq(adj) = 85.9%

4. Conclusions

Sintered density and hardness properties of graphite reinforced copper matrix composites has been investigated using a Taguchi orthogonal array design with different reinforcemnet concentration, compacted pressure and sintering temperature. The effect of composition is most significant compared to compaction pressure and sintering temperature on the sintered density of the specimens. Further, the hardness is more affected by the compaction pressure and sintering temperature. Experimental analysis revealed that concentration of graphite strongly affects average hardness, and the maximum hardness is found at 10 % wt. graphite.

References

[1] Goudah, G., et al. "Microstructural studies of sintered carbon nanotubes reinforced copper matrix composite", *Journal of Engineering Science and Technology*, 2010, 5 (3), pp 272 – 283.

[2] Zhen, J. M., et al. "Influence of graphite content on the dry sliding behavior of nickel alloy matrix solid lubricant composites", *Tribology International*, 2017, 114 (October), pp 322-328.

[3] Yang, H. J. et al. "Effect of the ratio of graphite/pitch coke on the mechanical and tribological properties of copper–carbon composites", *Wear*, 2010, 268 (11-12), pp 1337–1341.

[4] Powar, R. U. "Powder metallurgical processing and characterization of graphite particulate reinforced copper matrix composite", *International Journal of Research Science & Management*, 2015, 2 (6), pp 54-57.

[5] Gupta, S & Singh, G. "Fabrication of copper graphite composite material & its mechanical properties", *International Journal of Advance Research and Innovation Ideas in Education*, 2017, 3 (3), pp 347-362.

[6] Kumar, J & Mondal, S. "Microstructure and properties of graphite-reinforced copper matrix composites", *Journal of the Brazilian Society of Mechanical Sciences and Engineering*, 2018, 40, Article number: 196.

[7] Vairamuthu, J. et al. "Optimization of powder metallurgy parameters of TiC- and B_4C-reinforced aluminium composites by Taguchi method", *Transactions of the Canadian Society for Mechanical Engineering*, 2021, 45 (2), pp 249-261.

[8] Kucuk et al. "Optimization by Using Taguchi Method of the Production of Magnesium-Matrix Carbide Reinforced Composites by Powder Metallurgy Method", *Metals*, 2017, 7 (9), Art No. 352.

[9] Meignanamoorthy et al. "Evaluation on Powder Metallurgy Process Parameters of Ball-Milled AA8079-B_4C Nanostructured Composites via Taguchi Grey Relational Analysis", *Journal of Nanomaterials*, 2022, Art No. 7484053.

[10] Srinivas et al. "Microstructural, mechanical and tribological characterization on the Al based functionally graded material fabricated powder metallurgy", *Materials Research Express*, 2020, 7 (2), Art No. 026513.

Enhanced Deep Learning U-Net Model for Chest X-ray Image Segmentation

Asifuzzaman Lasker[a], Mridul Ghosh[b], Sk Md Obaidullah[a], Teresa Goncalves[c], Kaushik Roy[d] and Chandan Chakraborty[e*]

[a]*Dept. of Computer Science and Engineering, Aliah University, Kolkata-700160, India*
[b]*Dept. of Computer Science, Shyampur Siddheswari Mahavidyalaya, Howrah-711312, India*
[c]*Computer Science Department and ALGORITMI Center, University of ´Evora, Portugal*
[d]*Dept. of Computer Science, West Bengal State University, Barasat, Pincode-700126, India*
[e]*Dept.of Computer Science and Engg., National Institute of Technical Teachers' Training and Research, Kolkata-700106, India*
**Corresponding author, email: chandan@nitttrkol.ac.in*

Abstract

Modern healthcare uses chest X-ray images as an affordable medical imaging diagnostic resource. Lung segmentation is a fundamental feature of chest X-rays (CXRs) for screening and identifying lung conditions. It is difficult to segment the lungs on several patients' CXRs because they are opacified. The purpose of this paper is to resolve this issue by using a division formula based on U-Net. Our recommended design was developed by combining MobileNetV2 and InceptionResNetV2 pre-trained models. The segmentation performance of this architecture can be improved by using a stacked framework based on pre-trained models. In the analysis involving three widely-recognized datasets for lung segmentation, our method improved the accuracy by 2.52% in respect to dice coefficient and 2.37 % IoU over the traditional U-Net model.

***Keywords**:* Supervised localization, U-Net, Semantic Segmentation, Chest X-rays

1. Introduction

Radiographic diagnostics are performed all over the world on a daily basis, using a variety of imaging modalities. Among all imaging modalities, CXRs imaging is the most prevalent and economically viable method for diagnosing pulmonary conditions [1]. Lung segmentation is one of the most significant aspects of clinical support applications that evaluate respiratory disorders. By separating lung areas from adjacent tissue, lung segmentation indicates lung edges and areas. According to the published scientific article, deep Convolutional Neural Network (CNN) methods are used for both categorization and segmentation of diseases. A U-shaped framework has been designed with balanced encoding and decoding modules for capturing enhanced image information. U-Net-based frameworks were employed in this study to segment X-ray images based on upsampling and downsampling mechanisms. These architectures are very popular for medical image segmentation. According to the published scientific article [2], deep CNN methods are used for both categorization and segmentation of diseases. In the CNN approach, features are used for classification and the evaluation score reaches a considerable height. Considering the large amount of data required for the training process, pre-trained architectures were used to optimize CPU power and processing time. This allowed for increased efficiency in data processing while still achieving satisfactory results.

There are several factors that constrain image segmentation, including brightness, shade, noise, and object variations, making it a tedious and time-consuming part of biomedical technology. In segmentation, pixels are divided into distinct areas based on their features in the surrounding regions. In order to address this issue, researchers developed an automatic segmentation framework to identify infected lung regions [4-6]. The use of intelligent methods helps improve the detection and severity of many diseases at an early stage. It is quite difficult to employ several standards label and tag datasets in order to obtain the required algorithmic output for computer-based medical image segmentation. The process of pixel-based segmentation in CXR images, specifically for lung regions, frequently results in noise, making it challenging to obtain accurate annotations. The annotation techniques of individual annotators may lead to substantially different results between them, and significant interobserver disagreement may also exist. Several studies have applied a human-in-the-loop technique to minimize the annotation burden [7]. The annotations for algorithmically generated labels were manually checked and corrected by annotators in order to improve deep learning-based training and build a more reliable segmentation system. The effectiveness of deep learning over conventional methods has been documented in the literature [8]-[11]. To accomplish this, our study utilized standard U-Net architecture for segmenting the lung region from CXR images.

The contribution of the proposed work is listed below:

1. The proposed framework introduces an innovative stacked architecture that seamlessly integrates MobileNetV2 and InceptionResNetV2 with U-Net, significantly enhancing the accuracy of lung segmentation in chest X-rays.
2. A novel meta-learner component is developed, optimizing the fusion of features from pre-trained networks, resulting in a robust model that outperforms traditional U-Net frameworks.
3. The study contributes a standardized pre-processing protocol for chest X-rays, ensuring consistency across datasets and improving the model's training efficiency and generalizability.

2. Earlier Works

Commonly, imaging techniques such as X-ray, CT scans, and MRIs are utilized for diagnosing respiratory diseases. The method of segmentation usually incorporates criteria based on the treatment approach or the illness's progression stage, which is predominantly medical in nature. Regardless of the type of disease, patients receive additional supportive care alongside the primary treatment. Diagnoses are often enhanced by segmenting multiple organs and providing essential data to healthcare providers. A range of CNN models, including Fully-CNN, U-Net, and Mask R-CNN, as well as their various integrations, have been applied to the task of segmentation.

Lasker et al [12] suggested a computationally effective stacked ensemble architecture using a CNN network and three previously trained neural networks. The performance scores of three datasets are 97.28%, 96.50%, and 97.41%, respectively, and they show effectiveness of the architecture performed in those datasets, Ghose et al. [13] proposed an ensemble architecture for text/non-text image separation and represents the increase in performance of prediction score. Lasker et al. [3, 14] prepared a stacked ensemble architecture for CXR image segmentation depending on U-Net models. In U-Net models, it uses three DL architectures as an encoder module: MobileNetV2, InceptionResNetV2, and EfficientNetB0. In a study, the suggested framework was compared to the traditional U-Net model using the three available lung segmentation datasets.

Chatterjee et al. [15] developed a classification method based on unequally distributed classes to identify COVID-19 disorder using a different autoencoder (VAE). They carried out in-depth experimental analysis, and the results showed considerable advancements in COVID-19 detection. Lasker et al. [16] designed an efficient deep learning framework to extract deep features from photos. These features were then used to categories the images using various methods of machine learning. The highest accuracy rate achieved by the MLP-based classification approach is 96.81%. Gayathri et al [17] provided a technique that investigated thorough computer-aided diagnosis utilizing the CNN, autoencoder-based approach to identify disorders.

3. Architecture design

Our suggested system is built on a combination of MobileNetV2 and InceptionResNetV2, integrated with a U-Net structure. This U-Net design, which is tailored for splitting medical images into distinct sections, uses a layered CNN approach. It works in three main stages: initially reducing the image size, then refining the features at a reduced scale, and finally enlarging the image to its original size with improved segmentation.

The fusion of MobileNetV2 and InceptionResNetV2 in our model is a strategic choice aimed at harnessing MobileNetV2's lightweight structure and efficient depthwise separable convolutions for high-quality, channel-specific feature extraction from lung images. Concurrently, InceptionResNetV2's sophisticated design merges inception modules with residual connections, enhancing the model's capability to discern the complex variability in medical imagery while preventing the vanishing gradient issue. This synergy allows our integrated model to deliver a comprehensive segmentation of chest X-ray images, capturing an extensive array of features that range from the minutely detailed to the highly abstract, thereby bolstering the precision and dependability of lung segmentation, all the while optimizing computational resource use.

Within our model’s structure, the U-Net’s encoding component is integrated with two distinct pre-trained neural networks, forming a tandem system that benefits from a meta-learning process for prediction tasks. This meta-learning module comprises three dense layers with 32, 64, and 128 units respectively, and includes a dropout rate of 0.4 to avoid overfitting. Following the last dense layer, we introduced a batch normalization layer to stabilize learning. Finalizing this meta-learner's design required several iterations. We constructed a comprehensive system by individually creating U-Nets with MobileNetV2 and InceptionResNetV2 bases, and then amalgamating these models. To simplify the model, we adjusted MobileNetV2’s alpha parameter to 0.45. Moreover, we established a skip connection from the activation layer to enhance feature transmission. Different filter sizes 16, 32, 64, and 128 were used in the decoder part to maintain consistency with the encoder's skip connections. The complete structure of our proposed model is depicted in Figure 1.

To evaluate the model performance we used two readily accessible datasets [19] namely Shenzhen Hospital (SH), and Montgomery County(MC) in this research. In the datasets of MC, and SH, there are 138, and 662 original X-ray images and matching masks, respectively. There are two different resolutions of images in these databases: 4892 x 4020 and 3000 x 3000. To ensure uniformity of the input, all training images have been reduced to 256 X 256 resolutions to boost training performance.

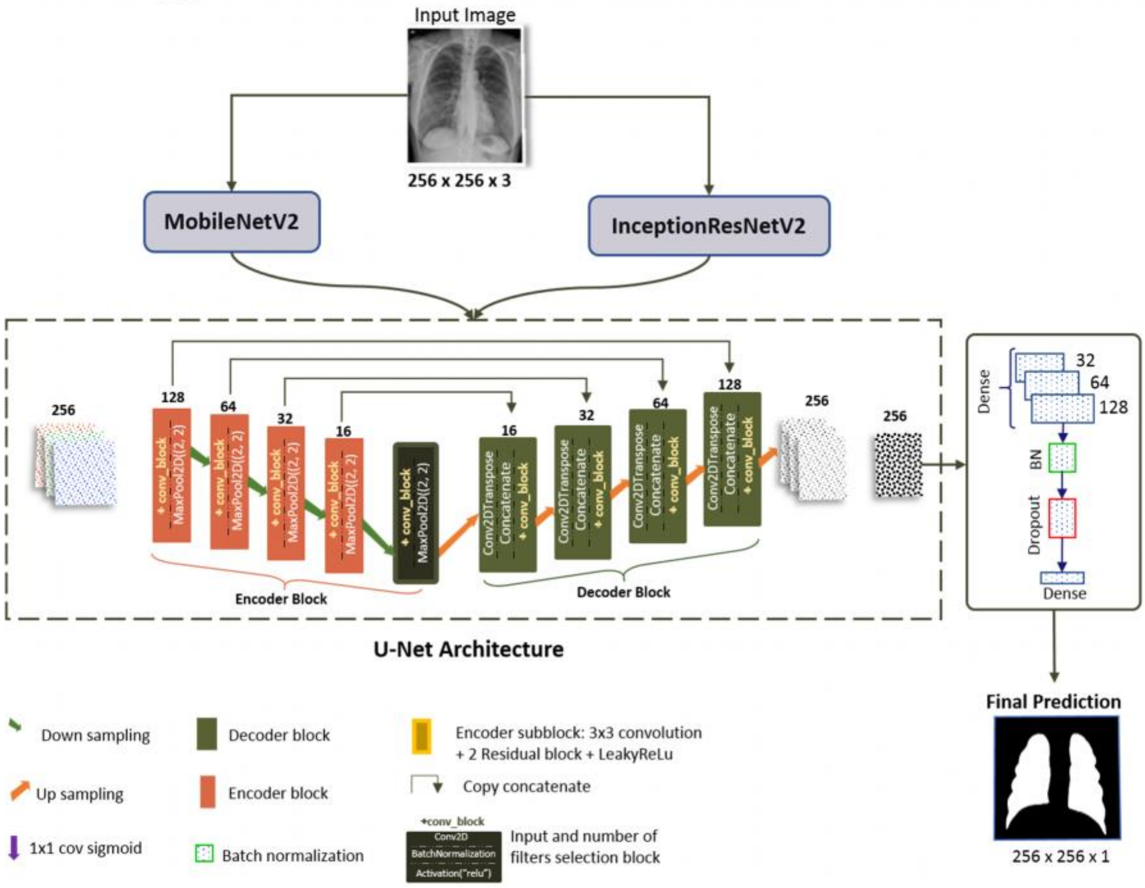

Figure 1: Proposed U-Net-based stack framework for lungs X-ray image segmentation

4. Evaluation protocols and results

4.1 Evaluation metrices for segmentation

To assess the accuracy of the segmentation, we employ the Dice Coefficient (DC) and the Intersection over Union (IoU) as key statistical measures. The computation of both DC and IoU involves considering the total area of the image (A) alongside the area identified by the segmentation process (S). Within the segmented area, we distinguish between the actual segment (S_t), which is the ground truth, and the segment predicted by our model (S_p).

$$Dice\ Coeff = \frac{2.A\,(S_p \cap S_t)}{A\,(S_p + S_t)} \qquad IoU = \frac{2.A\,(S_p \cap S_t)}{A\,(S_p \cup S_t)}$$

4.2 Training Regime

To enhance the performance of our model, we fine-tuned it by adjusting several hyperparameters. These included the batch size, the learning rate, and the number of training cycles, set at 16, 0.0001, and 50, respectively. When we compare this to the U-Net model, our model has 8.14%, and 0.10% fewer parameters than the U-Net combined with MobileNetV2 and U-Net combined with InceptionResNetV2 configurations. As for the processing speed, our model achieved inference times of 183 milliseconds for U-Net with MobileNetV2, 141 milliseconds for U-Net with InceptionResNetV2, and 149 milliseconds for the dual configuration. The impact of these hyperparameter adjustments is illustrated by four distinct learning curves, which are presented in Figure 2.

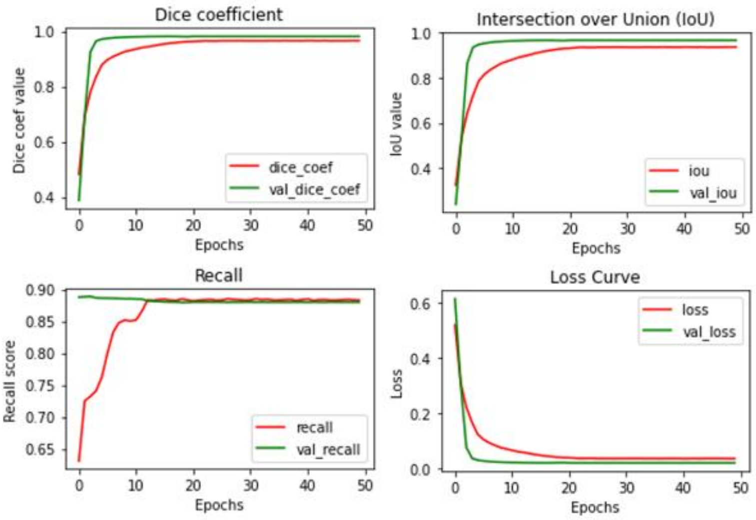

Figure 2: *The training curve for the U-Net with a two-stack model.*

4.3 Results

To assess the effectiveness of our segmentation process, we used five different measures for a comprehensive comparison across multiple model architectures. Details of these comparisons are provided in Table 1. The initial results are from the standalone U-Net model, followed by outputs when combined with MobileNetV2 and InceptionResNetV2 in a stacked arrangement. On datasets MC and SH, the combined framework improved the DC and IoU scores by over 2% compared to the standalone U-Net. Additionally, when examining three separate evaluations, it was observed that the U-Net's DC, IoU, and Recall metrics showed enhancement when it was integrated with the MobileNetV2 and InceptionResNetV2 models that had been previously trained. These improvements are also detailed in the corresponding sections of our report.

Table 1. Comparative outcomes using U-Net combined with different state-of-the-art architectures.

	Loss	**Dice Coeff**	**IoU**	**Recall**	**Precision**
U-Net	0.0259	0.9583	0.9376	0.8694	0.9876
U-Net | MobV2	0.0246	0.9673	0.9519	0.8948	0.9985
U-Net | IncepV2	0.0202	0.9712	0.9602	0.9101	0.9980
U-Net | MobV2 | IncepV2	0.0102	0.9832	0.9616	0.9356	0.9986

Note: MobileNetV2(MobV2), InceptionResNetV2(IncepV2)

After analysing the suggested model, the CXR image, original data, binary mask, and segmented lungs are shown in **Figure 3**. Third column (Binary Mask) indicates that the proposed systems work well with validation data.

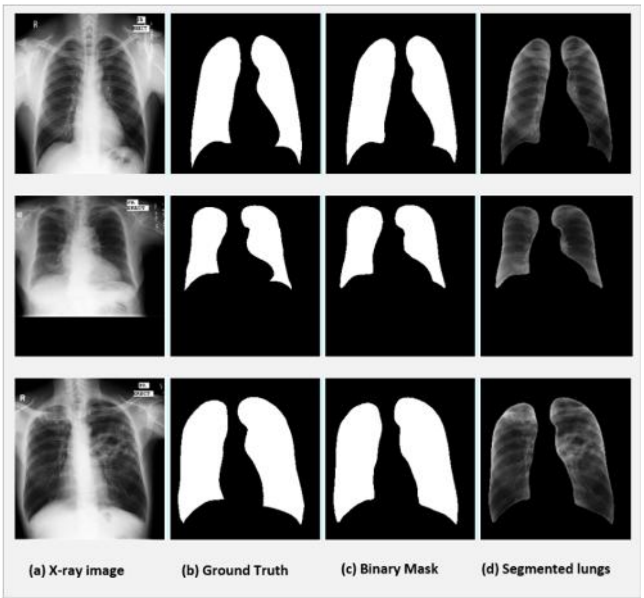

Figure 3: *The initial chest X-ray (CXR) images alongside the corresponding Ground truth, Binary Mask and segmented lungs.*

5. Discussion and Conclusion

This study successfully demonstrated the potential of a stacked architecture combining U-Net with MobileNetV2 and InceptionResNetV2 for lung segmentation in chest X-rays. However, it is crucial to acknowledge that the methodology carries inherent limitations. For instance, the model's reliance on a diverse yet finite set of public datasets could influence its generalizability across varied clinical scenarios and demographic profiles. Moreover, while the stacked framework has shown promising results, its computational demands may pose challenges in resource-constrained environments.

Our research has yielded a novel lung segmentation framework that leverages the strengths of U-Net in conjunction with the advanced feature extraction capabilities of MobileNetV2 and InceptionResNetV2. This stacked approach has demonstrated enhanced performance over individual models, as evidenced by the remarkable results obtained using multiple public datasets. The integration of these pre-trained networks into a unified architecture not only boosts segmentation accuracy but also paves the way for cost-effective and scalable solutions in medical imaging diagnostics. Despite these challenges, the findings from our research provide a strong foundation for future studies, encouraging the exploration of other segmentation models like DeepLab, SegNet, and Mask R-CNN. Our work not only contributes to the advancement of medical imaging technology but also opens new avenues for research that could lead to more sophisticated and nuanced approaches in biomedical imaging.

References

1. Mukherjee, Himadri, Priyanka Sreerama, Ankita Dhar, Sk Md Obaidullah, Kaushik Roy, Mufti Mahmud, and K. C. Santosh. “Automatic lung health screening using respiratory sounds.” Journal of Medical Systems 45 (2021): 1-9.

2. Lasker, Asifuzzaman, Sk Md Obaidullah, Chandan Chakraborty, and Kaushik Roy. "Application of machine learning and deep learning techniques for Covid-19 screening using radiological imaging: a comprehensive review." SN computer science 4, no. 1 (2022): 65.
3. Lasker, Asifuzzaman, Mridul Ghosh, Sk Md Obaidullah, Chandan Chakraborty, and Kaushik Roy. "Deep features for covid-19 detection: performance evaluation on multiple classifiers." In International Conference on Computational Intelligence in Pattern Recognition, pp. 313-325. Singapore: Springer Nature Singapore, 2022.
4. Mukherjee, Himadri, Bubai Das, Sahana Das, Ankita Dhar, Sk Md Obaidullah, K. C. Santosh, Santanu Phadikar, and Kaushik Roy. "Deep Neural Network for Pneumonia Detection Using Chest X-Rays." In Computer Vision and Image Processing: 5th International Conference, CVIP 2020, Prayagraj, India, December 4-6, 2020, Revised Selected Papers, Part I 5, pp. 78-87. Springer Singapore, 2021.
5. Saad, Mohd Nizam, Zurina Muda, Noraidah Sahari Ashaari, and Hamzaini Abdul Hamid. "Image segmentation for lung region in chest X-ray images using edge detection and morphology." In 2014 IEEE international conference on control system, computing and engineering (ICCSCE 2014), pp. 46-51. IEEE, 2014.
6. Abedalla, Ayat, Malak Abdullah, Mahmoud Al-Ayyoub, and Elhadj Benkhelifa. "Chest X-ray pneumothorax segmentation using U-Net with EfficientNet and ResNet architectures." PeerJ Computer Science 7 (2021): e607.
7. Shan, Fei, Yaozong Gao, Jun Wang, Weiya Shi, Nannan Shi, Miaofei Han, Zhong Xue, Dinggang Shen, and Yuxin Shi. "Lung infection quantification of COVID-19 in CT images with deep learning." arXiv preprint arXiv:2003.04655 (2020).
8. Ghosh, Mridul, Sayan Saha Roy, Himadri Mukherjee, Sk Md Obaidullah, K. C. Santosh, and Kaushik Roy. "Understanding movie poster: transfer-deep learning approach for graphic-rich text recognition." The Visual Computer (2022): 1-20.
9. Ghosh, Mridul, Gourab Baidya, Himadri Mukherjee, Sk Md Obaidullah, and Kaushik Roy. "A deep learning-based approach to single/mixed script-type identification." Advanced Computing and Systems for Security: Volume 13 (2022): 121-132.
10. Ghosh, Mridul, Somnath Chatterjee, Himadri Mukherjee, Shibaprasad Sen, and Sk Md Obaidullah. "Text/non-text scene image classification using deep ensemble network." In Proceedings of International Conference on Advanced Computing Applications: ICACA 2021, pp. 561-570. Springer Singapore, 2022.
11. Ghosh, Mridul, Himadri Mukherjee, Sk Md Obaidullah, K. C. Santosh, Nibaran Das, and Kaushik Roy. "LWSINet: A deep learning-based approach towards video script identification." Multimedia Tools and Applications 80, no. 19 (2021): 29095-29128.
12. Lasker, Asifuzzaman, Mridul Ghosh, Sk Md Obaidullah, Chandan Chakraborty, and Kaushik Roy. "LWSNet-a novel deep-learning architecture to segregate Covid-19 and pneumonia from x-ray imagery." Multimedia Tools and Applications (2022): 1-23.
13. Ghosh, Mridul, Somnath Chatterjee, Himadri Mukherjee, Shibaprasad Sen, and Sk Md Obaidullah. "Text/Non- text Scene Image Classification Using Deep Ensemble Network." In Proceedings of International Conference on Advanced Computing Applications, pp. 561-570. Springer, Singapore, 2022.
14. Lasker, Asifuzzaman, Mridul Ghosh, Sk Md Obaidullah, Chandan Chakraborty, Teresa Goncalves, and Kaushik Roy. "Ensemble Stack Architecture for Lungs Segmentation from X-ray Images." In International Conference on Intelligent Data Engineering and Automated Learning, pp. 3-11. Springer, Cham, 2022.
15. Chatterjee, Sankhadeep, Soumyajit Maity, Mayukh Bhattacharjee, Soumen Banerjee, Asit Kumar Das, and Weiping Ding. "Variational Autoencoder Based Imbalanced COVID-19 Detection Using Chest X-Ray Images." New Generation Computing (2022): 1-36.

16. Lasker, Asifuzzaman, Mridul Ghosh, Sk Md Obaidullah, Chandan Chakraborty, and Kaushik Roy. "Deep Features for COVID-19 Detection: performance evaluation on multiple classifiers." In International Conference on Computational Intelligence in Pattern Recognition, pp. 313-325. Springer, Singapore, 2022.
17. Gayathri, J. L., Bejoy Abraham, M. S. Sujarani, and Madhu S. Nair. "A computer-aided diagnosis system for the classification of COVID-19 and non-COVID-19 pneumonia on chest X-ray images by integrating CNN with sparse autoencoder and feed forward neural network." Computers in Biology and Medicine 141 (2022):105134.
18. Ronneberger, Olaf, Philipp Fischer, and Thomas Brox. "U-net: Convolutional networks for biomedical image segmentation." International Conference on Medical image computing and computer-assisted intervention. Springer, Cham, 2015.
19. "Tuberculosis chest X-ray datasets." National Libray of Medicine, 30 Mar. 2021, lhncbc.nlm.nih.gov/LHC-downloads/dataset.html.

Remarkable Contributions by Jaina Mathematicians in Ancient India

Kinsuk Giri*
Department of Computer Science & Engineering, National Institute of Technical Teachers' Training and Research, Kolkata, West Bengal, India

Debi Prasad Mishra
National Institute of Technical Teachers' Training and Research, Kolkata, West Bengal, India

**Corresponding author, email: kinsuk@nitttrkol.ac.in*

Abstract

We mostly consider on Jainism about their religious teachings, which indeed are very profound. However, Jainism also has a rich tradition in Mathematics. The main focus of the present article is to represent a brief outline on significant contributions of Jaina works on mathematics during ancient India, which were made during from BC 6th century to the AD 5th century.

Keywords: Ancient India, Mathematics, Jainsm, Sulbasutras, Infinity.

1. Introduction

The history of Indian civilization is segregated into three eras viz. ancient India (pre-hostoric – AD 500), medieval India (AD 500 – AD 1857) and modern India (AD 1857 - Present). The first ever enough indirect evidences of application in mathematics are obtained during the beginning of Indus Valley civilization (3000 BC) which lasts up to next 1000 years (*Srinivasiengar*, *1967*). Aryans entered India after the Indus civilization collapsed around 2000 BC and founded the Vedic civilization. Fortunately, the first ever evidence related to Indian culture that includes mathematics is revealed during this Vedic civilization. The word *ganita*, which literally means the science of calculation, first appears in Vedic era. Nevertheless, to be mentioned that the word *Ganita* equivalent to the word mathematics in Indian context. During the post-Vedic period, Buddhism and Jainism experienced a surge in popularity in India. Jainism is not only religion but also a philosophy. Around 600 BC, Jainism was founded in India. It became the dominant religion in the Indian subcontinent and made significant contributions to the development of Jaina mathematics. Important mathematical works during Jaina period were developed and discovered from around 300 BC to 400 AD (*Sykorov*, *2006*). The chronology of the history of ancient Indian mathematics is not actually linear. Many evidences show that the work of one group of people is proceeded by the work of another group and so on. However, In Fig.1, a tentative chorology in context of ancient Indian mathematics is given for obtaining the overall idea. It is true but sad fact that the contributions of mathematics during ancient Indian period are highly neglected by rest of the mathematics community. In addition, ancient Indian contributions on mathematics and astronomy are unfortunately underrated compare to the contributions made by Egyptians, Babylonians, and Arabians. It is relevant to mention here that the mathematics at Ancient India was the highest in the world until the beginning of 17th century.

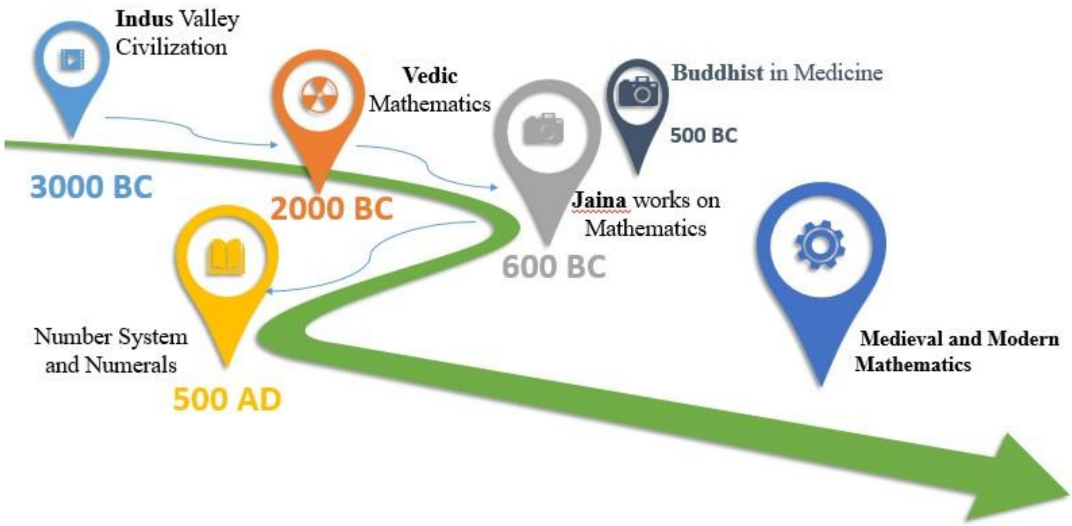

Figure 1*: Schematic Diagram of Ancient Indian Mathematics Timeline*

2. Significant Contributions of Jain Mathematics

Jainas of ancient India took keen interest in the study of mathematics as this was treated as an integral part of their religion. A number of Jaina texts of mathematical importance have been analysed by various groups while a number of scripts yet to be studied due to damage conditions of the manuscripts. Tens of Prajnapti and Sutras (canonical literature) were revealed from time to time. Few of these are Jambu Dwipa PrajnaptiSthananga Sutra, Surya Prajnapti, Uttaradhyayana Sutra, Anuyoga Dwara Sutra and Bhagwati Sutra. Ganita-sara-samgraha which was written by Mahavira (AD 850), written by the founder of Jaina religion, was himself a mathematician.

2.1 Themes of Jain works in Mathematics

Jain mathematicians sought to provide evidence for these beliefs through rigorous study and logical proof. According to Jainism, time and the universe are both infinite. They aimed to demonstrate the endless nature of time, life, and the universe using mathematical principles. There were ten separate themes (*Dutta, 1929*) on the work of then Jain mathematicians. These are:

i. *vyavahara* (subjects of treatment)
ii. *parikarama* (fundamental operation)
iii. rajju (geometry)
iv. *kalasavarna* (fractions)
v. *rasi* (heap, mensuration of solid bodies)
vi. *varga* (quadratic equations)
vii. *yavat-tavat* (simple equation)
viii. *ghana* (cubic equations)
ix. *vikalpa* (permutations and combinations).
x. *varga-varga* (biquadratic equations)

The exact meaning of some of the above themes is not properly revealed. Although, few controversies are there, still maximum themes of Jain mathematics are significant and meaningful. In the light of all available texts and evidences, few of the above themes are discussed in this article as below:

2.2 Measuring Huge Distance and Time

Prior to Jain's era, mathematics was primarily used for practical purposes such as trade, astronomy, and religion, and was limited to dealing with small numbers. The concept of infinity was not yet incorporated into existing mathematical methods. Jain mathematicians approached this problem by making a fundamental assumption: to reach the highest place, one must first ascend to higher levels, and then continue to ascend even further. Only then can one reach vast distances, including infinity. As a result, they began their work by attempting to find large numbers using established units and concepts. The thinking process of Jains, as illustrated in Figure 2, is based on the assumption that if their God travels one lakh Yojana (equivalent to ten lakh kilometres) with in one second, subsequently the God will travel the said distance within six months is called a Rajju. It is worth noting that this distance is equivalent to 15,552,000,000,000 kilometres, which is the distance travelled by light in 60 days (Dutta, 1929).

Figure. 2*: Concept of Huge Numbers by Jains (Human image courtesy: www.hermesstaffing.com)*

Similarly, we can give another example that Jains thought at this era in connection with the discovery of *Pallya. According to their theory, a pot with a length, breadth, and depth of one Yojana each is filled with a hair collected from a sheep at every century.* The total time it takes to fill the pot is referred to as one Pallya (Kaye, 1929). Assuming an average hair length of five centimetres and a volume of 0.0001 cubic centimetres, the pot's volume would be 1000000000000000000 cubic centimetres. Therefore, one Pallya would be equivalent to 1,000,000,000,000,000,000,000,000 years. This is an incredibly long time!

2.3 Different types of Counting Proposed by Jains

Jainism employs following three types of numbers for counting (Hayashi, 1995):

- ✓ Sankhyat (countable)
- ✓ Asankhyat (countable but infinite) and
- ✓ Anant (endless and not countable)

To represent large numbers, Jain mathematicians developed a new number writing method using index numbers, which involve raising small numbers to powers. The term 'Ardhacched' refers to the number of times a number can be divided by 2 without leaving a remainder. For example, the Ardhacched of 524288 is 19, as this number can be divided by 2 nineteen times. Similarly, 1162261467 can be written as 3 raised to the power of 19, making the Trikacched of this number 19. In other words, 2 raised to the power of 19 equals 524288. Correct formulas for both of the combinations and permutations are seen clearly in Jaina works. Few of these formulas for combinations and permutations are given below.

$$C_1(n) = n, \quad C_2(n) = \frac{n(n-1)}{1 \cdot 2}, \quad C_3(n) = \frac{n(n-1)(n-2)}{1 \cdot 2 \cdot 3}.$$

$$P_1(n) = n, \quad P_2(n) = n(n-1), \quad P_3(n) = n(n-1)(n-2)$$

Jains developed the method that helps to find the concept of combinations. This was termed by them Meru Prastara. This involved forming an early version of Pascal's triangle using the following formula.

$$C_r(n+1) = C_r(n) + C_{r-1}(n)$$

Around 10th century AD, a the then commentator explained *Meru Prastara* in a nice way (*Datta and Singh*, *1935*). To begin, draw a square. Then, draw two squares below it, starting from the mid position o of the bottom side. Repeat this process, drawing three squares below the previous row, and so on. In the top square, write the number 1. Additionally, in each row, write the number 1 inside the first and last squares. For every other square, write the summation of the numbers in the form of two squares above it that overlap it. In figure.3 the same been illustrated. It is unfortunate that French mathematician Pascal discovered the same thing Jains *Meru Prastara* and gave a nomenclature as *Pascal’s Triangle*. However, actually Pascal’s Triangle was discovered by Jains before 2000 years ago of French mathematician Pascal.

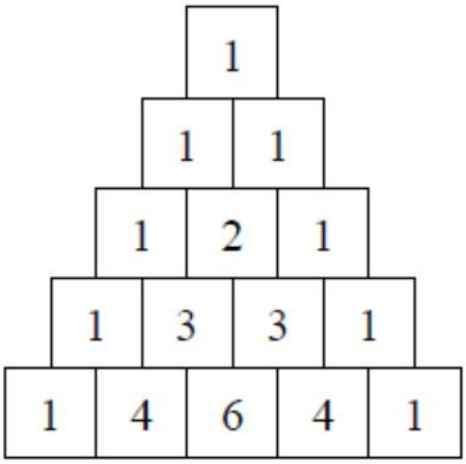

Fig.3: *The diagram Meru Prastara given by Jains*

2.4 Discovery of the Idea of Infinite Number

The Jaina sages used extensive time and effort to solve problems involving large numbers, and eventually developed a method for approximating infinity through calculation. Their initial approach was to take the largest number imaginable, denoted as A, and then square it to obtain A squared. Take this as B. Now repeat the process to obtain B squared. Continue this pattern to approach infinity.

Later, they gave systematic proposal which is given below. In Fig.4, we tried to visualize these steps.

- ➢ Take a wide pot as the similar size of earth and count mustard seeds in it.
- ➢ Even when the pot is full, you still won't be able to reach the highest number.
- ➢ If you repeat the process with a pot that is one thousand times larger.
- ➢ It will still be smaller than the highest possible number.
- ➢ A symbol was needed to represent this quantity that does not stop.

Hence, consequently the concluded that "*The term used to describe a number that is larger than any number that can be imagined or calculated by the human mind is called ASEEM or INFINTY*".

Figure.4: *Concept of Infinity by Jains. The image of mustards with wooden spoon is taken from www.amazon.in and the globe image is taken from www.dreamstime.com*

2.5 Mensuration Formulae given by Jains

There are several evidences in support of works on Mensuration by Jains. It is clearly seen at the book *Tattvartha Sutra* (also called *Tattvarthadhigama Sutra*) a book written bu Umaswati *(Sarasvati, 1979*). Umaswati's work is the earliest comprehensive Jain philosophy text that is accepted as authoritative by all four Jain traditions. It was the first Sanskrit language text on Jain philosophy. Umaswati stated the following formulae for the mensuration of a circle in his book (*B. S Jain, 1987*).

- Circumference of a Circle © = $\sqrt{10 * d * d}, \boldsymbol{d} = length\ of\ diameter\ of\ the\ circle$
- Area of a Circle = $\frac{1}{4} * C *$d

  If a = arc of a segment of a circle, c = its chord and h = its height, then

- $ch = \sqrt{4 * h * (d - h)}$
- $h = \frac{1}{2}(d - \sqrt{d^2 - c^2})$
- $a = \sqrt{c^2 + 6h^2}$
- $d = \frac{1}{h}(h^2 + 0.25c^2)$

2.6 Values of π by Jains

In Greek Alphabet, the sixteenth letter Pi (π), is most widely known mathematical constant. It is well known that it equals the ratio between circumference and diameter of any circle (π = C/D). The value of π had been reported in Jaina mathematics at the various number of research works *(Gupta, 1986; Jha & Jha, 1990)*. In Sulabasutras, it was reported that the value of π as 18 * (3–2√2) = 3.088. It is also founda at Manava Sulabasutra that the value of π to be 28/5= 3.125. According to Baudhayayana Sulabasutra, the perimeter of a pit is three times its diameter, which leads to an approximation of the value of π as 3. Moreover, the ancient Jaina school of mathematics preferred the approximation π = √10.

3. Concluding Remarks

The ancient Jain mathematicians from India were very sophisticated with respect to their wisdom and knowledge. This is relevant to mention here that the Jain mathematicians had a deep understanding of the concept for defining an extra ordinary large number which is later termed as infinity. Apart from that they also worked on mathematical progressions, power indices etc. This article highlights the need for further research in an uncharted area. Jaina mathematics, which is over two thousand years old, may provide insight into the foundations of mathematics. Hence, we should reveal these in order to honour this rich mathematical heritage.

References

1. B. Datta, The Bakhshali mathematics, The Bulletin of the Calcutta Mathematical Society, 21, 160, 1929.
2. B. S. Jain, Contribution of Ancient Jaina Mathematicians, Deshbhushanji Maharaj Abhinandan Granth, 1987
3. C. N. Srinivasiengar. The History of Ancient Indian Mathematics, World Press Private Ltd., Calcutta, 1967
4. B. Datta, A. N. Singh, History of Hindu Mathematics (part I), Lahore: Molital Banarsidass, 1935
5. I. Sykorova, Ancient Indian Mathematics, WDS'06 Proceedings of Contributed Papers, Part I, 7–12, 2006
6. G. R. Kaye, The Bakhshali Manuscript, Archaeological Survey in India, New Imperial Series XLIII, vol.I, Parts I-II, Central Publication Brand, Calcutta, 1927
7. R. C. Gupta, Madhavacandra's and other octagonal derivations of the Jaina value π = √10, Indian J. Hist. Sci. 21 (2) (1986), 131-139.
8. Sarasvati. Geometry in Ancient and Medieval India. Indological Publ., Delhi, 1979
9. S. K. Jha and M. Jha, A study of the value of π known to ancient Hindu & Jaina mathematicians, J. Bihar Math. Soc. 13 (1990), 38-44.
10. T. Hayashi, The Bakhshali Manuscript: an ancient Indian mathematical treatise, Groningen, 1995

The Alchemy of Wootz Steel Production In Ancient India

N. Anantha Krishna*
Department of Mechanical Engineering, MBU, erstwhile SreeVidhyanikethan Engineering College, Tirupati, A.P

Debi Prasad Mishra
National Institute of Technical Teachers' Training and Research, Kolkata, West Bengal

*Corresponding author, email: nanathakrishna@vidyanikethan.edu

Abstract

These days, the mystical alchemy of generating a 'damask' pattern on ultra-high carbon Wootz has gathered much research attention. Anachronistic technologies emerged during the evolution of ancient Indian civilizations due to the constant development of ancient technical marvels. These advancements spurred society and cultures to adapt humanity to the history of technology. The history of Indian technology can be traced back to prehistoric periods, with different thought-provoking pieces of evidence, one of which is transmutation. Ancient Indian Alchemy advocated transmuting base metals into gold to synthesize metallic medicaments and elixirs that resolve many rampant and morbid diseases. As a result of the transmutation of multilevel structures of materials from atomic to coarse level, alchemy tries to create a distinct material with specific attributes. In this work, the alchemy of Wootz developed in India, such as pyro-technology, quenching, and detoxification procedures.

1. Introduction

Technology that is now considered anachronistic arose alongside the growth of ancient civilizations as a result of the ongoing development of ancient technical marvels. These improvements encouraged nations and cultures to introduce humans to the development of technology. One such marvel is Wootz. Wootz was coined when European travellers from the 17th century onwards came Anachronistic technologies arose with the advent of ancient civilizations as a result of continuous advancement in technical marvels of antiquity across its making, in southern India. Wootz is the Anglicization of 'Ukku', the Kannada word for steel. Wootz was the Anglicization of 'Ukku', the Kannada word for steel. In this regard, comparable to how Wootz was esteemed in ancient India, Bintie was a steel of high regard in ancient China. It was manufactured in China or imported from India or Central Asia. Diverse opinions exist regarding its composition; some contend that it was merely Indian Wootz steel, while others assert that it was a locally produced steel of indigenous origin Also, it was discerned as a type of iron that was produced in ancient China by a process called "direct reduction" [1]. Many researchers found that India was burgeoning in producing colossal quantities of this world-famous Wootz steel during those times, and the fame for this steel was mustering much attention [2]. The technology of making high carbon wootz steel by crucible processes consummated in Southern parts of India is a preeminent pyro-technological and pyro-metallurgical achievement investigated by several researchers [3]. A complex thermo-mechanical procedure involving forging and annealing transforms them into magnificent steel cakes.[4]. In this regard, making sword blades from wootz steel with an idyllic interior design is also an unparalleled feat. Accordingly, few researchers attributed this as a feat of Quantum black smithy [5]. They laid sufficient evidence for such ingenious quantum-level marvels in a multi-scale materials architecture [6]. In that domain, quantum design triumphed, employing the best materials, expertly manipulating elements and compounds, and outperforming mediaeval alchemists' fantasies. [7]. Accordingly, Seventeenth-century Damascus sabers revealing cementite nanowires and carbon nanotubes stirred several speculations. The researchers investigated and deliberated on vital mixes involving organic molecules, specific metal catalysts, diverse ores, and unique components. [8]. Due to interfusion, heat cycling, and cyclic forging, the components above eventually consolidate into planar arrays parallel to the forging plane, encouraging the growth of nanotubes and the formation of cementite nanowires and coarse cementite particles. These changes gave the metal very significant mechanical properties. In this connection, early Swiss metallurgist and professor Zschokke was fortunate enough to obtain a few wootz blades for the research. In his book, Manfred Sachse details a portion of Zschokke's findings on some of the mechanical properties such as hardness, bending toughness etc and general composition of those samples [9]. While the historical methods of Wootz steel production did not meet modern environmental requirements, certain aspects of the process may be deemed environmentally beneficial.

The use of natural elements such as iron ore and carbon rich additions derived from organic sources such as leaves or wood demonstrates a commitment to sustainability. Further, the methods involved in crafting Wootz steel were intricate and often carried out by skilled artisans in smaller quantities. The process required careful attention to detail and specific conditions for the carbonization and quenching phases. As a result, while Wootz steel was highly prized for its exceptional qualities, including strength and sharpness, its production volume was likely limited. The demand for Wootz steel might have been met within certain regions or specialized markets, but specific evidences on production in quantities that could fulfil large-scale requirements, such as those seen in contemporary industrial steel production remain unclear, which can be given significant research attention. Because of the apparent similarities in their origins, few researchers believe that specific recipes exist. These formulas derive from Indian alchemy. In antiquity, blacksmiths, alchemists, and astronomers all presented convincing proof. The consummate inferences parallel present characterisation approaches using only naked-eye observations on metals, fires, and phase transitions [3]. As a result, techniques and recipes based on ancient Alchemy ideas are likely to be included.

2. Pyro-technology in Ancient Indian Alchemy

Transmutation is an intriguing piece of evidence demonstrating the origins of Indian technology in prehistoric times. Its primary goal is to transform a substance's dynamic potential by eliminating any inherent contaminants A 14th-century text, "Rasendra Sara Sangraha," describes the macro analysis of metallic specimens and how to analyze them by their luster and form of the fractures. This shows the state of the art in alchemy in the 14th century. [10].

Metals in medicines date back to Sushruta (400 AD). However, its supremacy was significantly propounded in the 8th century, particularly during the Tantric period of the 9th century. Indian alchemy (Rasavada) came to full speediness during the 10th-14th centuries. Over the time, numerous inorganic materials piled into their Materia Medica, and many Pyro-metallurgical procedures were heaped into their texts [11].

Hence, Indian alchemy deals with the alchemical and biopharmaceutical transmutation of minerals, metals, and herbs. It majorly encompasses the Purification procedures of materials as mentioned above, and their calcination process. After serious pyro-technical procedures, metals transform into inorganic compounds, mostly identifiable as simple oxides. It is unknown if any organometallic complexes form in them during this process. If one observes a zinc sample after calcination, it consists of 87.2% zinc oxide and 0.6% potassium. This was not an easy procedure as for zinc, and the texts usually prescribe 10-12 incinerations. With this, one can estimate typical heat treatment procedures adopted by the ancients in transforming metal into the internal administrable form [12].

Pyro-technology forms a strong background and core constituent in the incineration and calcination. Blacksmiths were taught some of these procedures and used them to quench their weapons, even in blood and urine [13]. Their quenching methods seem to take inspiration from alchemical procedures like *Nirvana* (hardening) and *Dravikarana* (liquefication) [14]. Arrow quenching procedures and heat treatment of ancient surgical instruments are good evidence. B. Prakash gave a detailed description of the construction of furnaces, classification of iron and steel, design, composition, and process of marketing crucibles by referring to ancient Indian alchemical texts [15].

In the 17th Century, modern chemistry was emerging from alchemy, and fire science was in an infant stage, during which German chemist J.J Becher (1635-82) and Stahl (1660-1734) collectively proposed Phlogiston (in Greek Phlogiston is the fire of earth) theory. It emphasizes that any flammable material contains Phlogiston, liberated as smoke, heat, and light, where weight loss is another indication. They also proposed that all solid materials contain Phlogiston in variable proportions, and as a result, they exhibit differentiation in burning. Lesviev Wood cock regards Gibbs's free energy as a phlogiston alternative, and prior to 1850, all scholars of science believed in caloric theory till the initiation of thermodynamics. Based on Joseph Black's concept of Phlogiston's absolute Levity C.E Perrin summarised the framework as follows: Phlogiston is ponderable, imponderable and weightless, and Phlogiston has absolute levity. The Greek's concept of Phlogiston as the fire of earth, its escape from the body in a whirling motion, and its relation with air can also be found in ancient Vedic references as Agni (Fire God).The 34 names of Agni mentioned in the very old Sanskrit thesaurus Amarakosha more or less speaks the same properties of Phlogiston. MM. Vineland DE Morveau laid some lines of thought proposing that Phlogiston does not gravitate towards the earth's centre; instead, it rises, and hence an increase of weight in metallic calx is found. The alchemists believed that every material contains (molten fluid and vitreous earth). The idea of the levity of Phlogiston seems to originate from the ancient idea of the levity of fire. Aristotle also held this old view by Indian alchemists where matter/ substances were characterized by elements [16-18].

Matter/substances can be arranged from fixed to volatile, with fire at the top; Pythagorean's fourth tetractys of simple bodies also lays the same material scale. They assigned the monad, which is fire in the first tetractys, as the most volatile, followed by the duad, which is air (less volatile than fire), and finally water and earth as triads and tetrads (more fixed than those mentioned above). They proposed that elements be classified based on their tenuity and density. According to Samkhya philosophy, the five elements (air, water, earth, fire, and void) are among the nine categories that comprise a substance (the remaining four being time, space, self, and mind). These elements, or panchabhutas, can comprehend objects in the natural world. This proposal is also known in Greek philosophy. This was first proposed by Empedodes (492-432 BC), and it was later popularised by Aristotle (384-322 BC). Panchabhutas (integrating ether/Akasha) was the Indian term for it. These five elements are also classified as three gunas: sattva, rajas, and tamas. Other than Indian alchemy, their equivalent western alchemical terms refer to them as three philosophical principles: salt, sulphur, and mercury, as explained in detail in Bhojas Works [19]. Few researchers look into the ancient classification of a substance based on its taste and the dominant elements receding in it. Asthtangahridaya's Vagbhatta created 20 attributes of a substance and their equivalent mapping to each element that form tags in a part-whole schema [20]. In other words, all materials used to manufacture wootz-type Damascus steels can be classified as Sattva, Rajas, and Tamas; among them may be materials containing flammable earth-Rajas or philosophical sulphur.

3. The Alchemy of Wootz

Wootz steel was earlier produced in India by introducing carbon into the crucibles in wood or organic additions. Table 1 indicates the presence of carbon content in percentage from different wootz objects as notified by B. Prakash et al. [15]. Specific elements, such as iron and carbon sources such as wood or leaves, are combined in the carbonization process of Wootz steel. In a controlled atmosphere, the mixture is heated, allowing carbon to infuse into the iron. This critical phase leads to Wootz steel's particular qualities, such as its strength and sharpness. Specific elements, such as iron and carbon sources such as wood or leaves, are combined in the carbonization process of Wootz steel. In a controlled atmosphere, the mixture is heated, allowing carbon to infuse into the iron.

In Wootz steel manufacture, the carbonization process is critical to producing the correct composition and properties. However, the first in-detail analysis of Wootz in the middle of the 19thCentury indicated 1.33% of combined carbon and 0.312% of uncombined carbon [21]. Also, this, along with metallic catalysts and organic additions, gave rise to nano carbon tubes as speculated by few researchers: such inclusions and detoxification recipes much prevailed in Ancient Indian Alchemy, which is discussed in the next session. The transformation of Indian Wootz into a Damascus blade is depicted in Figure 1, and the idyllic pattern in Figure 2.

Table-1 *Carbon composition in wootz steel objects (Source: B. Prakash [15])*

Sl. No.	Object	% C	Reference No.
1	*Ingot*	1.64 to 1.68	14 P.82
2	*Wootz swords*	1.33 to 1.87	14 P.82
3	*Swords*	1.1 to 1.8	14 P.82
4	*Wootz (Srilanka Origin)*	1.97	26 P.390
5	*Wootz (Indian Origin)*	1.64	26 P.390
6.	*Wootz (Indian Origin-Mysore)*	0.45-0.9	26P.390

Wootz was synthesized from the carbonization of wrought iron, heated in closed crucibles with specific ingredients over the fire, and operated with bellows. The operation was repeated to remove excess carbon, and the entire process took several hours to complete. In some parts, quenching and mystic quenchants were also employed. It was a highly pure iron with 1.5% carbon. The cakes were shipped to several parts and forged to swords, which displayed an idyllic pattern, as shown in Figure 3. Herein, the hypereutectoid level plays a significant role in exhibiting such luster due to the alignment of cementite particles during cooling. The unique internal microstructure was replete with bands of small cementite particles along the band's centre line.

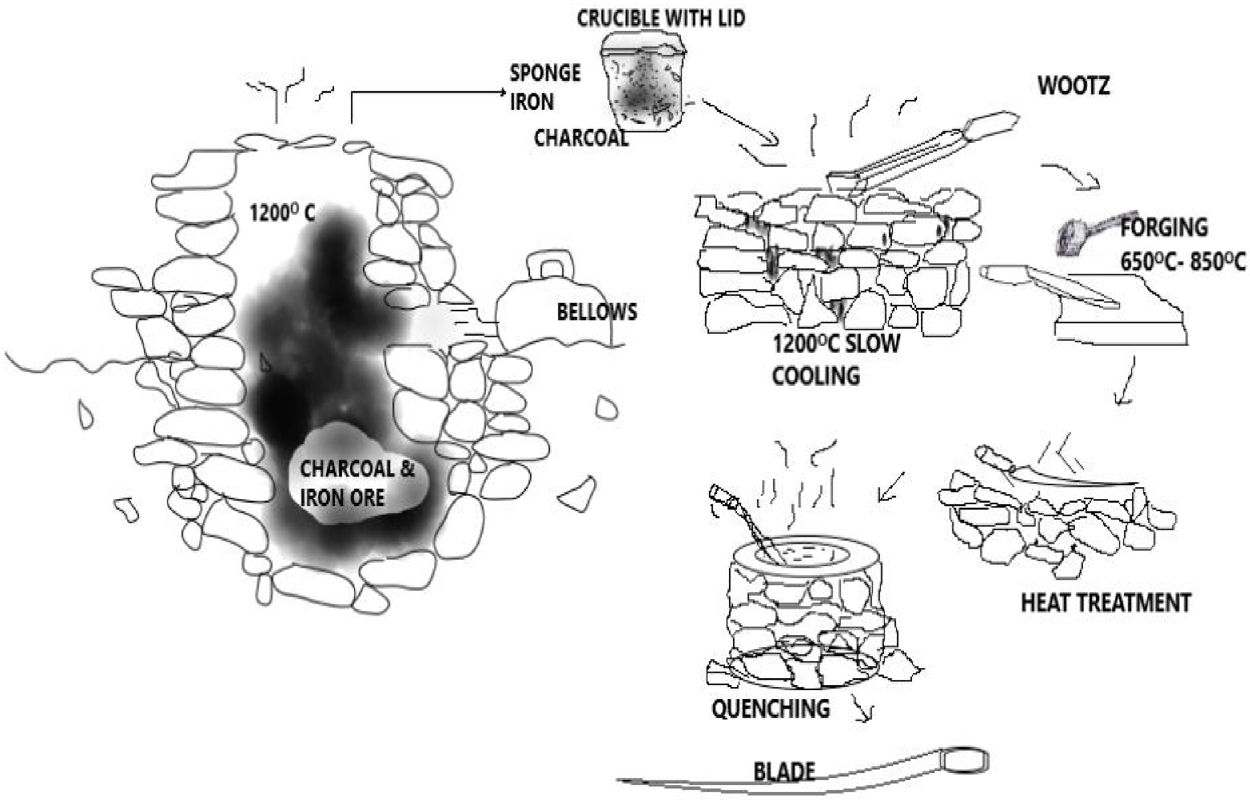

Figure 1: *Manufacturing of blades from Wootz (Source: A.K Biswas [22])*

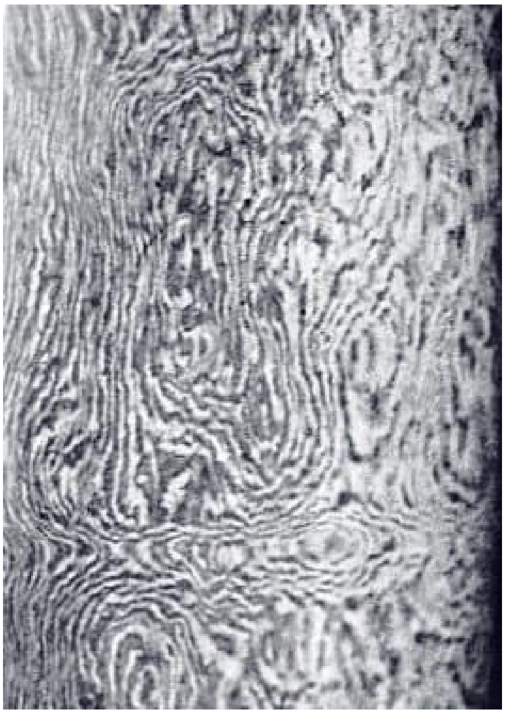

Figure 2: *Unique banding patterns on Wootz (source: Wikipedia)*

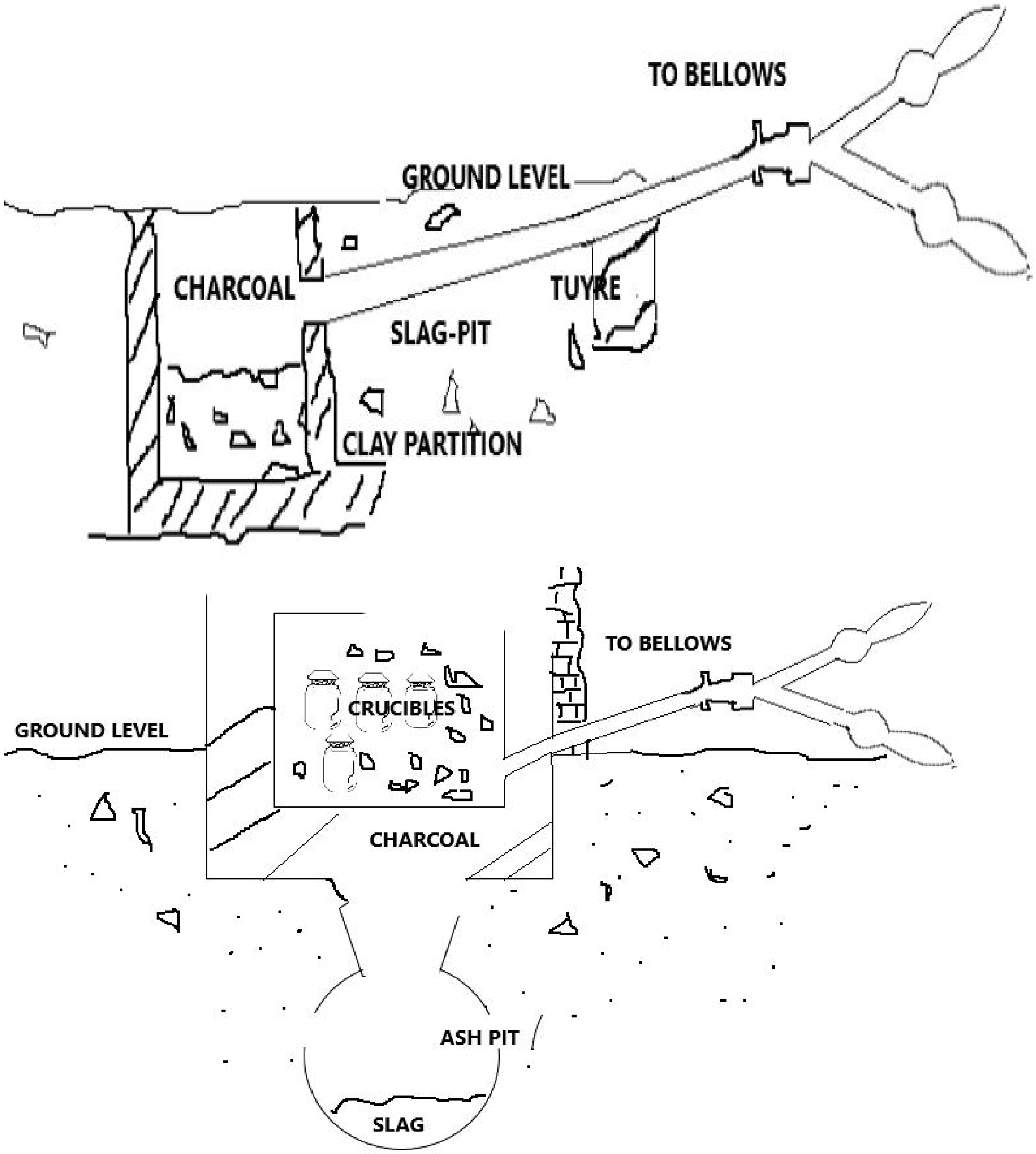

Figure 3: *Pyrotechnology-Crucible furnaces for wootz steel (Source: B. Prakash [15])*

The structure is a function of the heat treatment process but was essentially found in pearlite. The bands were found to be aligned parallel to the plane of forging, and further manipulation of his angle produced a variety of intricate patterns. According to recent research, ultra-high carbon steels have superplastic properties because the pro eutectoid cementite network microstructure forming along the grain boundaries of earlier austenite may result in a finer distribution of spheroidised cementite particles in a fine matrix. The two typical processes in vogue are presented in Table 2.

Table 2: *Wootz steel manufacturing process*

Sl. No.	Process	Details	Remarks
1.	*South Indian Process*	Crucibles charged with Wrought iron + 5-10 % of wood charcoal (in % wt) of *Cassia Auriculata*, and 1 to 2% of leaves of *Calotropis gigantic* (called *avaram* in Tamil), and the mouth was sealed with clay. The charge was covered with one or two leaves of plants like *Convolvus laurifolia* or *Asclepias gigantea.* or *Tandra tegga*(in Telugu) with leaves and rice husk. The crucible is then sealed with a sun-dried clay lid or a ball of moist clay.	a) Crucibles were covered with charcoal in dome fashion. b) Foot-operated drum bellows were vogue in central India. c) In large hand bellows, buffalo/goat skin blowers were involved. d) Typically, 20 to 25 crucibles under 1450ºC to 1550ºC for 6 hours. e) Solidified wootz ingots reveal thick cementite plates in transformed ledaburite and pearlite matrices. f) Quenching was done in moist clay, dry sand heap, and throwing water.
2.	*Hyderabad Process*	Large pine-shaped granite clay crucibles with ground pieces of oil, rice husk, grog closed with a ball of clay and lid.	a) Steel was produced by refining white cast iron with 2.5% carbon by the chemical action of highly oxidizing fayalite slag. b) During decarbonization, some dephosphorization was noted. c) The furnace was a double chambered furnace with ground level pit. d) Molten metal was allowed to solidify in the furnace. e) Composition: Carbon 1.68%, Silicon 0.43%, Phosphorus 0.02% and Sulphur 0.2%.

4. Purification and detoxification procedures in Indian Alchemy

C.S. Smith emphasizes that an overarching structure occurs due to hierarchy and anarchy of smaller parts at different levels of structures- structure, substructure, and superstructure. Accordingly, two possible dissymmetrical interplays arise between the surfaces of part and whole. Hence, all things are interactive – both up and down the scale of clumpings. Specifically, the hierarchical alteration between a material's externally noticeable attributes/traits and an internal structure responsible for it occurs at all levels and applies to all things [23]. Specific pyro-technological processes, quenching techniques, quenchant recipes, and detoxification or purification procedures may enhance such possibilities. Pre-treatment of raw materials in extractive metallurgy and preparation of metallic medicines was considered the most crucial part of Indian Alchemy. It is known as "Samskara," and the ancient Indians believed that this process transmutes a substance's latent attributes, which leads to the summation of new ones. Numerous modes of such treatments are stated in Indian alchemical texts, such as Svedana (Boiling), Mandhana (churning), Mardana (grinding), Bhavana (impregnation), Nirvana (heating and quenching in prescribed mediums) etc. Some of them are shown in Figures 4(a) and 4(b) used for detoxification and particle size reduction. The Ancient quenching techniques are believed to be developed out of mysticism, empirical experimentation and intervention of some typical quenchant recipes. A few pieces of historical evidence are shown in Table 3.

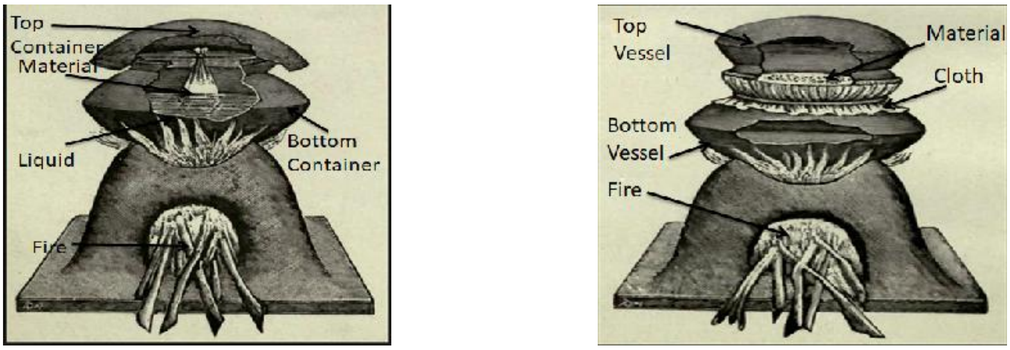

Figure 4: *(a) Swedana Yantra and (b) Dola Yantra [24]*

Table 4 highlights some of the material treatments involved in Indian Alchemy. Each treatment is a distinctive method for the specified raw material. It is believed that subtle changes in materials can be brought by some arduous purification and detoxification procedures that radically transform the chosen material.

Table 3: *shows significant Quenching indications in the Historical Period pre-Christian Era India [25]*

Sl.No.	Time line	Quenching details
1.	*528 BC*	At Ujjain Site, large varieties of offence equipment,slags, fluxes, water jar-indicative of quenching
2.	*600-300 BC*	At Jajamau site, Quenched and tempered axe with laminated structure at the edge
3.	*3rd Century BC*	At Pandu RajarDhibi, Sharp cutting edge sickle with a tempered martensitic structure
4.	*2nd Century BC*	At Ror, Kangrasite,Rapidly quenched ferrite and martensite plates on Iron razor

L.A Chernozatonsk II et al., investigated the conditions for generating nanotube structures in cavities innate in metal matrices. It is found that treatment modes and composition are significant factors in the generation of the same. Few researchers studied the possible mechanism involved in generating such tiny structures. It is found that metal particles enable the ousting of carbon and hydrogen at cooling from melt into the discontinuities [25]. C.Y Jagtap et. al. worked on purification and detoxification procedures w.s.r to Copper in Medival Indian alchemical medicine; it elucidates several metallurgical phenomena like hydrogen embrittlement, nano crack forming, and bio-beneficiation, as innate aspects of the traditional Indian Alchemical recipes- especially *Nirvapavis-a-vis quenching* [26-27]. Specific coatings were applied on crucibles mentioned in Ancient Indian Alchemical Pyro-metallurgical works. Few researchers studied thermogravimetric analysis of such coatings [28]. During such processes, two-dimensional interfaces give a separate identity of things in three dimensions. Also, inter-dimensional interaction gives the very essence of form, and uniformity of tiny particles' relationship to their neighbor [6]. Further, the boundaries are the source of inchoation for both strengths and weaknesses and provide a solid basis for any crystalline change's inception. With the reduction in temperature, hydrocarbons decompose under the catalytic influence of nanoform. Besides, nanotubes in pores are formed in carbon vapor at temperatures below 1200^{0}C. The flow collides the micropore's surface in the breakneck cooling matrix, and bulker fragments are deposited first crack offshoots. Hence, nano entities take in particles of a lesser mass, further becoming the nuclei of nanoarrays on which lighter particles are deposited after supplementary cooling [29-30]. CNTs were synthesized involving pretreated plant materials – heat treatments in the air for partial carbonization – and a low-temperature cyclic oxidation process in the presence of air.

Table 4: *Indian Rasavada material treatments*

Sl.No.	Material Treatment	Method	Material mediums
1.	*Nirvapana*	Heating and Dipping into liquid Medium.	Acidic(*Triphala decoction*),Alkaline(lime water),Oils and milk
2.	*Dhalana*	Heating for melting the metal or semi-metal and dipping in a liquid medium	*Churbidaka*(lime water),Ghee and Milk
3.	*Urdhvapathana*	Sublimation and distillation	Paste of Acidic medium like Lemon juice
4.	*Adhahpathana*	Sublimation and distillation	Paste of Acidic medium like Lemon juice
5.	*Bharjana*	Frying	Ghee
6.	*Bhavana*	Tirturation	Garlic, ginger, salts, Lemon juice
7.	*Virechana*	Cleansing and sifting	Usually Seeds are used
8.	*Shoshana*	Shade dryed	Usually Seeds are used
9.	*Mardana*	Rubbing	Juices or Salts or Decoctions
10.	*Sthapana*	Soaking in the liquid medium	Cows –Urine , Lemon Juice
11.	*Svedhana*	Boiling or fomentation	Steam of water or milk, Lemon Juice,
12.	*Avapa*	Keeping metals in melted media	Special herbs like *Devadali*
13.	*Shodhana*	Include one or all above mentioned procedures	All Materials including metals and minerals
14.	*Marana*	Incineration	Metals and minarals including *Mardana* materials

5. Conclusion

In conclusion, the transmutation of wootz steel as an art form with quantum-level forging emerged in India with the nanoscience of nanotechnology or material science but drew considerable attention as a novel material. Although many of the wootz-making recipes appear to be riddled with mysticism and speculative experimentation, a growing body of literature on ancient Indian Alchemy, pyro technology, quenching, and other detoxification procedures mentioned in it emphasizes the transmutation of the material hierarchy to achieve any novel material. Depending on the alchemical selection and characterization of elements, organic additives, and catalysts most likely created an idyllic miracle.

References

1. W. L. Bintie: the wootz steel in ancient china, Indian Journal of History of Science, 44.3, 369-388, 2009.
2. S. Srinivasan and S. Ranganathan, India's Legendary wootzsteel : An Advanced Material of the Ancient World, Tata Steel, 2004
3. O. D. Sherby and J. Wadsworth, Ancient Blacksmiths, the Iron Age, Damascus Steels and modern metallurgy, Journal of Materials Proceeding Technology, 117, 347-353, 2001.
4. O. D. Sherby, and L. Wadsworth, Damacus Steels, Scientific American, p. 118, 1987
5. S. Srinivasan and S. Ranganathan, India's Legendry Wootz Steel: An advanced Material of the Ancient World, Tata Steel
6. C. S. Smith, Structure, Substructure and Superstructure, Reviews of Modren Physics, 1965
7. G. B. Olson, Designing a New Material World, Pathways of Discovery, 288, 2000.
8. M. Reibold, P. Paufler et al., Discovery of Nanotubes in Ancient Damascus Steel, Physics and Engineering of New Materials, 2009
9. J. Wadsworth, Archeometallurgy related to swords. Materials Characterization. 99:1-7, 2015
10. G. K. Bhatt, Rasender Sara Samgrah, Choukhambha Sanskrit Sansthan, Varanasi, 2007
11. S. C. Sankhyadhar, D.Sankhyadhar and R. Nighantu, Chaukambha Orientalia, Varanasi, 2010
12. R. C. Kapoor, Some observations on the metal-based preparations in the Indian Systems of Medicine, Indian Journal of Traditional Knowledge 9,562-575, 2010
13. D. S. Mackenzie, History of Quenching, Advanced Materials and Process, 2015
14. Y. C. Jagtap, P.K. Prajapati, R. Patil and Y. S. Chowdary, Therapeutic uses of Tamra (Copper) bhasma – A review through BhaishajyaRatnavali, 3,128-135, 2014
15. B. Prakash, Ferrous Metallurgy in Ancient India, Metallurgy in India: A Retrospective, 52-91, 2001
16. A. Rorsch, Climate science and the phlogiston theory, Energy & Environment · Vol. 18, No. 3+4, 2007
17. M. Caamano, A Structural Analysis of the Phlogiston Case, 70:331–364, 2009
18. D. Allchin, J. Hutton and Phlogiston, Annals of Science, 51:6, 615-635, 2014
19. M. Roy, The Concept of Yantra in the Samarangana – Sutradhara of Bhoja, Indian Journal of History of Science 19, 118-124, 1984.
20. A. Balkrishna, Ashtanga Hridayam, Divya Prakashan, 2014.
21. P. Neogi, Iron in Ancient India, Prathibha Prakasan, 2007
22. A. K. Biswas, Minerals and Metals in Ancient India, D.K. Print World 1, 1996
23. C. S. Smith, A Search for Structure, MIT Press, Cambridge, 1981
24. P. Rây and P. C. Rāy. "History of chemistry in ancient and medieval India: incorporating the History of Hindu chemistry." *(No Title)* (1956).
25. L. A. Chernozatonski, V. P. Val Chuk et al., Synthesis and Structure investigations of Alloys with fullerene and nanotube inclusions, Pergamon, 35: 6, 749 – 753, 1997
26. C. Y. Jagtap, B. J. Patgiri and P. K. Prajapati, Purification and Detoxification procedures for metal *TAMRA* in Medical Indian Medicine, Indian Journal of History and Science, 48.3,383-404,2013.

27. S. Mitra, S. Gupta and P. K. Prajapati, Role of media in Shodhana process w.s.r to metals/minerals, Indian Journal of Ancient Medicine and &Yoga, 2, 211-217, 2009
28. N. A. Krishna et. al., A Critical review on Ancient Alchemical Metal Treatment Procedures in Rasagrandhas and Brhadvimanika Shastra, Materials Today: Proceedings, 2015
29. X. F. Xie, B. Goodell et. al., A method for producing carbon nanotubes directly from plant materials, Forest Products Journal, 59 (1): 26-28, 2016
30. J. Wadsworth, Archeometallurgy related to swords. Materials Characterization. 99:1-7, 2015

Architectural Elegance Through Time: Unveiling the Unique Construction Legacy of Hindu Temples in Ancient India

Samirsinh P Parmar*
Department of Civil Engineering, Dharmasinh Desai University, Nadiad, Gujarat, Bharat

Debi Prasad Mishra
National Institute of Technical Teachers' Training and Research, Kolkata, West Bengal, India
**Corresponding author, email:* spp.cl@ddu.ac.in

Abstract

Each epoch possesses a discernible construction methodology, inherently unique and emblematic of the prevailing ideologies, cultural progress, artistic inclinations, and architectural prowess of its particular civilization. From a nuanced standpoint, Hindu Temples stand out as embodiments of knowledge, artistic brilliance, architectural magnificence, and cultural legacy, symbolizing the pinnacle of building technology in the ancient Indian subcontinent. The timeless principles and customs of Indian Temples go beyond historical boundaries, echoing deeply in the present context, thereby sustaining the flexibility of traditional Indian values and wielding a significant effect on the socio-economic tapestry of society. This scholarly work delves into the intricacies of temple styles, design principles, geometric configurations, structural systems, and the intricate construction technologies intrinsic to Indian temples. The exposition meticulously unfolds the distinctive architectural styles and elements inherent in Hindu Temples. Furthermore, a comprehensive elucidation of the geometric design principles that underscored Indian temple construction is expounded upon within this discourse. The paper meticulously delineates the construction technology, commencing with the meticulous assembly of adept teams, through the stages of meticulous planning, intricate carving, and culminating in the seamless assembly of individual components.

Keywords: Ancient Indian Temple, Geometry, Geometrical Design Philosophy, Component parts, Symbolism, Vaastu planning, Elements of temple architecture, Fractal geometry, Fractal design.

1. Introduction

Hindu temples, referred to as Mandirs in Hindi, find their etymological roots in the Sanskrit word "*Mandira*." Despite variations in architectural styles across India, the fundamental essence of the Indian temple remains consistent. The architectural concept of temples in India took shape about 4500 years back, during the developed phase of the Indus-*Saraswati* or Harappan Civilization (2600-2000 BCE) [1]. Initially, these temples were outdoor shrines located under consecrated trees and/or near water source structures. However, a significant shift occurred during the Mahajana pada period (700 BCE), marking the emergence of the temple as a closed structure. The modest thatched huts in the villages of Northern India from 700 to 500 BCE served as initial prototypes for temple construction. [2]. The construction of multiple stories temples gained momentum during the *Sunga-Kusana* era (200 BCE-200 CE) [3]. The idea of dualism in Bhakti, which emphasizes the holy link between the deity and the devotee, gained prominence after the fall of the Gupta Empire in 320 CE. [4]. This conceptual shift led to the provision of two distinct spaces within the temple: the *garbhagriha* for the idol and the Mandapa for the devotees. An early illustration of this arrangement can be observed in the Sanchi Buddhist temple [5]. In the late fifth and early sixth centuries, during the Gupta period, Indian temple architecture underwent a significant transformation, breaking away from the limitation of vertical monumentality and introducing features like a second story and *shikhara* or *vimana* [6]. Interestingly, no mortar was used in the construction of these temples. During this time, temple iconography and architecture developed, with myths and gods being meticulously carved into stone and becoming essential elements of the temple's construction. [7]. Temple architecture developed in a unilineal form up until the fifth century, but by the seventh century, a regionalized style had taken hold.

The South Indian, or Dravida, style adopted a stepped *Vimana* that ended in a round '*stupi*', while the North Indian, or *Nagara*, style accepted a curved *shikhara* that terminated in a pointed finial. [8]. Modern temple erection in North India has become further diverse, while South India, Gujarat, and Orissa continue to adhere to traditional practices. Indian temples symbolize both the macrocosm (universe) and the microcosm (inner space), aiming to establish a connection between man and God [9]. Hinduism's central idea is that the temple, with its architecture, ornamentation, and ceremonies, is a location where one might achieve ultimate nirvana.

Indian temples promote the advancement of the arts and intellect as well. In the past, public courts, hospitals, and schools were located within temple complexes. Spacious halls were also used to recite epics like the Ramayana and the Mahabharata. [10]. The temples sustained themselves through income generated from assigned cultivable land, influencing the economic life of the community and providing livelihoods for many. This paper aims to offer a comprehensive overview of Indian temple style, design, geometry, structural systems, and construction technology [11]. It explains how Indian temples' resilience to seismic forces is derived from an exploration of the affiliation between structural solidity, symmetry, and proportion.

2. Architectural Styles of ancient Indian temples

Over the course of centuries, the architectural styles of ancient Indian temples have undergone a transformative evolution, influenced by a myriad of factors including geography, culture, history, and regional nuances. These distinct styles represent the diverse and dynamic nature of India's rich architectural heritage. The formation of the different architectural styles can be attributed to the factors like, geographical diversity, cultural influences, historical changes, artistic innovations, and availability of different construction materials. Table 1 depicts different styles of architecture of ancient Indian temples and its specific characteristics over an Indian map.

Table 1: *Architectural Styles of ancient Indian temples and its characteristics.*

Sr. No.	Architectural Style	Region	Characteristics	Prominent Temples and Examples
1	Nagara Style	Primarily in North India	Towers with curvilinear spires (shikhara), square sanctum (garbhagriha), and mandapa.	Prominent in temples of North India, especially in the Himalayan region.
2	Dravidian Style	Predominantly in South India	Towering gopurams (entrance towers), large and open mandapas, axial alignment of shrines, and elaborate sculptural work.	Prominent in temples of Tamil Nadu, Karnataka, Andhra Pradesh, and Telangana.
3	Vesara Style	Deccan region	A fusion of Nagara and Dravidian styles, characterized by a central tower with elements of both square and circular plans.	Prominent in temples of Maharashtra and parts of Karnataka.
4	Maru-Gurjara Style	Western India, especially Gujarat, Rajasthan	Elaborate and intricate architecture, often with domes and toranas (arched gateways).	Prominent in temples like the Dilwara Temples in Mount Abu.
5	Vijayanagara Style	Associated with the Vijayanagara Empire in South India	Large and ornate structures, intricate carvings, and pillared halls.	Prominent in temples of the Vijayanagara period, including the Virupaksha Temple in Hampi.
6	Hoysala Style	Southern Karnataka	Star-shaped platforms, sculpted walls with intricate detailing, and lathe-turned pillars.	Prominent in temples like the Chennakesava Temple in Belur.
7	Kalinga Style	Odisha (Orissa)	Pyramidical towers (rekha deula), sculptures depicting stories from epics, and a focus on intricate carvings.	Prominent in temples like the Lingaraja Temple in Bhubaneswar.
8	Chalukya Style	Associated with the Chalukya dynasty in Karnataka	Flat roof structures, carved pillars, and ornate sculptures.	Prominent in temples like the Badami Cave Temples.
9	Pallava Style	Tamil Nadu	Rock-cut architecture, monolithic structures, and sculptural decorations.	Prominent in temples like the Shore Temple in Mamallapuram.
10	Gandhara Style	Northwestern regions of India	Influenced by Greco-Buddhist art, featuring Greek and Roman architectural elements.	Prominent in early Buddhist monuments.

3. Steps in Temple Construction

Temple construction in ancient India involved a meticulous process guided by religious, architectural, and cultural principles. The steps in temple construction reflect the intricate craftsmanship and spiritual significance associated with these sacred structures.

1. **Site Selection:** Choosing an auspicious location was paramount. Vaastu Shastra, an ancient Indian architectural science, provided guidelines for selecting a site based on factors like direction, topography, and energy flow.

2. **Foundation Laying:** The foundation, often symbolic of the temple's stability and endurance, was laid with precision. Rituals and prayers accompanied this crucial step.

3. **Planning and Design:** Temple architects, often influenced by regional styles, religious beliefs, and royal patronage, created detailed plans encompassing layout, proportions, and decorative elements. The design incorporated spaces for sanctuaries, halls, and intricate sculptures.

4. **Materials Selection:** The choice of materials was crucial. Stone, particularly sandstone and granite, was commonly used for its durability. Wood and metal were also employed. The quality of materials influenced the temple's longevity.

5. **Sculpture and Carving:** Skilled artisans sculpted intricate reliefs and statues depicting deities, mythological stories, and celestial beings. Each carving was imbued with spiritual symbolism and aesthetic finesse

6. **Construction of Main Structure:** The construction of the main temple structure involved careful assembly of stones or bricks, following the architectural plan. Temples often featured a central sanctum (*garbhagriha*), a hall (*mandapa*), and a tower (*shikhara* or *vimana*).

7. **Ornamentation:** Elaborate ornamentation enhanced the visual appeal. This included decorative motifs, friezes, and intricate carvings adorning both the interior and exterior surfaces.

8. **Installation of Deities:** Once the main structure was complete, a consecration ceremony (*prana pratishtha*) took place to infuse spiritual energy into the temple. Images or idols of deities were installed in the sanctum.

9. **Ritual Consecration:** The consecration involved elaborate rituals conducted by priests to invoke divine blessings and sanctify the temple. This marked the formal commencement of worship and religious activities.

Temple construction was not merely a physical endeavour but a spiritual and communal undertaking. The careful adherence to religious principles, adherence to traditional craftsmanship, and the infusion of cultural symbolism contributed to the creation of magnificent and enduring structures that remain architectural wonders today.

The construction stages of ancient Indian temples are listed below as per the ancient Sanskrit texts.

i. **Selection of Location and Soil Examination (*Bhu Pariksha*):** This stage involves meticulously examining and choosing a fertile land with suitable soil for the construction of the temple and the surrounding town.

ii. **Material Selection for the Image (*Sila Pariksha*):** At this phase, the focus is on selecting and examining the appropriate materials for creating the temple's sacred image.

iii. **Crop Cultivation and Purification (*Karshana*):** Prior to construction, a specific crop, such as corn, is grown in the designated area. The harvested crop is then fed to cows, signifying the readiness of the location for town or temple construction.

iv. **Ritual for Divine Favor (*Vaastu Puja*):** This involves a ritual to appease Vaastu Devata, seeking divine favor and blessings for the upcoming construction.

v. **Removal of Undesired Elements (*Salyodhara*):** In this stage, any undesired elements, such as bones, are carefully excavated from the site.

vi. **Laying the Foundation Stone (*Adyestaka*):** The commencement of construction begins with the laying of the foundation stone, symbolizing the initiation of the temple-building process.

vii. **Foundation Ritual and Construction (*Nirmana*):** Following the foundation stone, a purification ritual is performed by sprinkling water mixed with auspicious substances. A pit is dug, filled with gems, minerals, seeds, and more, marking the actual commencement of the temple's construction.

viii. **Placement of Top Stone (*Murdhestaka Sthapana*):** This stage involves placement of the top stone over architectural elements like the *prakara* and *gopura*. Before the apexes are placed, special voids containing jewels, minerals, and seeds are formed.

ix. **Installation of Main Deity's Vessel (*Garbhanyasa*):** A vessel made of five metals (*pancaloha kalasa sthapana*) is ceremoniously mounted at the location designated for the main deity.

x. **Temple Construction Completion (*Sthapana*):** The main deity is formally installed, marking the completion of the temple construction.

xi. **Infusing Life into the Deity (*Prana-Pratistha*):** In the final stage, the main deity is consecrated and infused with divine life and essence.

4. Components of Hindu Temple Architecture

The Hindu temples established a distinct architectural structure in the latter half of the 7th century, and the fundamental elements in their original Sanskrit scripts are outlined as follows:

The primary enclosure of the temple is known as '*Vimana*', consisting of two parts [12]. The upper section of the Vimana is termed Sikhara, while the lower part within the Vimana is referred to as *Garbhagriha* (cella or internal chamber) (refer to Figure 1 (a) & (b)).

1. **"Shikhara"** denotes the spire or tower, shaped in a pyramidal and tapering form, symbolizing the mythical "Meru" or the highest mountain peak.

2. **“Garbhagriha”** is the womb chamber, the inmost section of any temple where the deity exist in. It is mainly square in plan and is accessed through the eastern side.
3. **“Pradakshina Patha”** represents the auxiliary pathway for walking around, which consists of an enclosed passageway outside the garbhagriha. Devotees walk around the deity in a circular clockwise direction to offer their homage
4. **“Mandapa”** is situated in front of the garbhagriha, the pillared hall, serving as an assembly point for pilgrims to chant, meditate, or observe the priests performing rituals.
5. In some instances, a **“Natamandira”** is provided, representing the hall for dance. In early temple structures, the ‘*mandapa’* was sometimes a separate and isolated structure from the sanctum.
6. **“Antarala”** designates the intermediate space connecting the main sanctum and the pillared hall of the temple premises.
7. **“Ardhamandapa”** refers to the front entrance at the main entry of the temple leading to the main temple. Some additional essential basic elements specific to South Indian temples include:
8. **“Gopurams”** are monumental sequence of pyramidal shaped domes and ornate entrances to the temple premises.
9. **“Pitha”** signifies the plinth height and type of the main temple.
10. Gateways distinctive to temples of North Indian regions are termed **“Toranas.”**

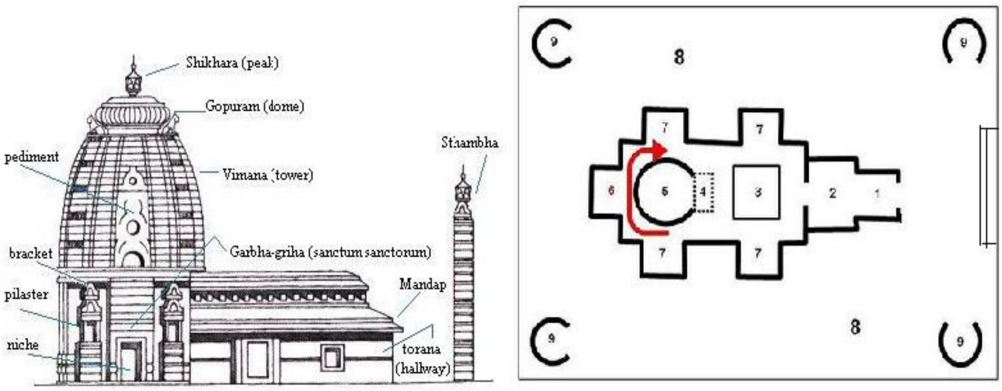

(a) Cross Sectional View

(b) Plan of Typical Hindu Temple

1. Ardha mandapa 2. Mandapa 3. Mahamandapa
4. Antarala 5. Garbh Griha 6. Pradakshina
7. Transepts 8. Jagati 9. Subsidiary shrines

***Figure 1:** Typical Elements of Hindu temples. (Source: https://en.wikipedia.org/wiki/Hindu_temple)*

5. Comparison between Architectural Styles

The distinct architectural designs of Hindu temples have undergone evolution driven by significant variations in geography, climate, culture, ethnicity, history, and language between the northern plains and the southern peninsula of India. Primarily classified based on natural features, Hindu temples can be broadly categorized into three main orders: the Nagara or 'northern' style, the Dravidian or 'southern' style, and the Vesara or hybrid style found in the Deccan region, serving as an intermediary between the other two. Additionally, peripheral regions such as Waste Bengal, Kerala, and the States within Himalayan range give rise to unique and regional styles. Table 2 provides a comparative analysis of distinctive features between the Nagara and Dravidian architectural styles.

Table 2: *Contrasting the Architectural Styles of Nagara and Dravidian Temples (Reproduced from [13])*

Particulars	***Nagara style architecture***	***Dravidian style architecture***
Temple's main spire (*Shikhara* Style)	'*Sikhara'* above temple	The Vimana, possibly having multiple levels (talas), with its uppermost part referred to as the shikhara
Mandapa spire (tower)	Certainly	Not at all
Shape of the spire	Curvilinear above the sanctum, as well as a straight-edged pyramidal structure	Straight pyramidal or, at times, curvilinear pyramidal, positioned over the shrine
Garbhagriha (Sanctum)	Ground storeyed or multi-storeyed	Usually, singular (though the Vimana may consist of multiple storeys)
Design	*Mandapa*, temple, and tower plans primarily exhibit a *Chaturasra* (four-sided) layout, with occasional variations such as '*Ashtasra*', '*Vritta*', '*Ayatasra*', '*Ayata Ashtasra*', '*Ayata Vritta*', '*Hasti Prishta*', and '*Dwayasra Vrita*'.	similar, as well as Prana *Vikara*
Gopuram (monumental entrance tower)	Not a protruding feature	A distinctive feature, though not imperative; post-10th century, frequently taller than the V*imana*. Multiple towers may be present on all borders of the complex, functioning as milestones for pilgrims.
Other topographies	Sacred ponds, fewer pillared '*mandapas'* within the temple grounds (with a separate *dharmshala*), '*prakara'* walls are uncommon, and the temple may have a single or multiple entrance.	Sacred ponds, numerous pillared '*mandapas'* within the temple grounds, *prakara* walls became prevalent, and the temple may feature a single or multiple entrance.
Foremost sub-styles	*Latina, Phamsana, Sekhari, Valabhi*	Tamil (upper and lower Dravidadesa), Karnata, Andhra
Regions	Northern, western, and central regions of the Indian subcontinent	southern parts of the Indian subcontinent, southeast Asia
Time line of enduring stone-masonry monuments	Late Kushana period, early Gupta: basic architecture; 6th-10th century	Late Gupta period: elementary; 6th-10th century: zenith

6. The Geometric Design of Hindu Temples

The *Vastupurashamandala's* geometry was designed to embody the concept of *Purusha* within the abstract notion of the square as the highest geometric form [14]. In this geometric representation, the square symbolizes the earth, while the circle embodies the cosmos, symbolizing endlessness and infinitude (refer to Figure 2). The mandala itself is a square subdivided into minor squares, forming a grid that represents different areas dedicated to respective deities. A commonly employed mandala involves subdividing the square into 64 and 81 squares [15]. Consequently, the *Vastupurashamandala* served as the foundational blueprint for the ground floor plans of Hindu temples. The temple's basic shape was derived from this mandala, with the outermost ring of squares defining the thickness of the main shrine's walls. The central squares were reserved for the most significant god, the inner loop of 12 squares formed the garbhagriha's walls, and the remaining 16 to 28 squares created the "*pradkshina patha*." These simple square divisions, through permutations and combinations, paved the way for the creation of more intricate temple compounds.

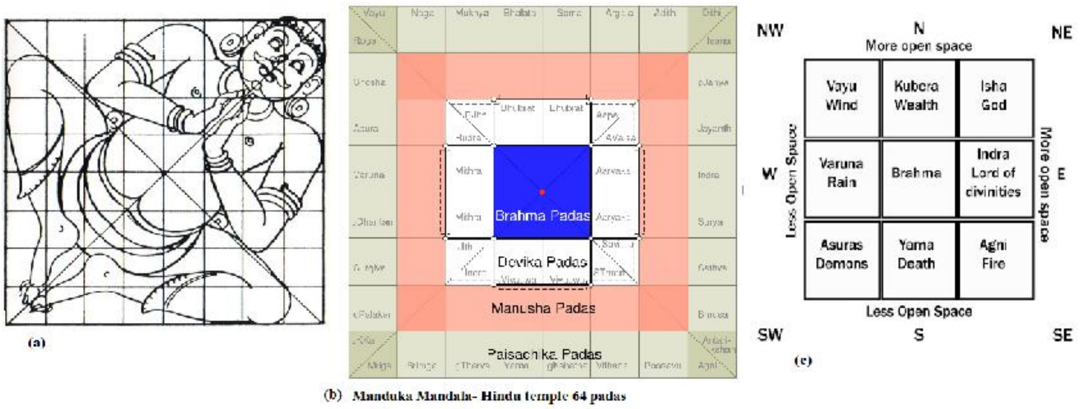

Figure 2: *The image of Vastupurushamandala with 64 blocks designated for diverse deities (Source: https://en.wikipedia.org/wiki/Hindu_temple)*

7. Fractal Characteristics in Temple Architecture:

The ancient Shani Mantra portrays the principles of the Sanatana Vedanta philosophy, as outlined below:

This *Purnam Shanti mantra* (पूण शान्ति मंत्र) is from '*Isha Upanishad'* and is one of the foremost principles of the *Sanatana dharma*.

ॐ पूणमदः पूणमिदं पूणात्पुणमुदच्यते
पूणस्य पूणमादाय पूणमेवावशिष्यते ॥
ॐ शान्तिः शान्तिः शान्तिः ॥

The connotation of shloka is, "*Supreme Being (Parmatma) is complete. It doesn't depend on any external agency for anything. Our Atman is a fragment of this infinite Supreme Being; hence our Atman is also complete and has the same characteristics as those of Parmatma. Our Atman is a replica of the Parmatma. The Supreme Being is infinite (अनंत). Hence, when a small fragment is taken out of it, it still remains complete" [10].*

In accordance with the ancient Indian *Sankhya* School of Philosophy, the cosmos is space-time harmonic simulation [16]. This implies that the cosmos's structure reproduces itself in a self-similar manner at progressively smaller scales. Similar to a hologram, each piece of the universe is self-contained, encapsulating all the information of the entire cosmos. The entire cosmos can be envisioned within a microlevel cosmic entity referred to as *Pinda-Brahmanda*. This fractal architecture is evident in various parts of the temple, including the shikhara (both in plan and front view), temple design, mandapa ceiling design, column design, and more (see Figure 3).

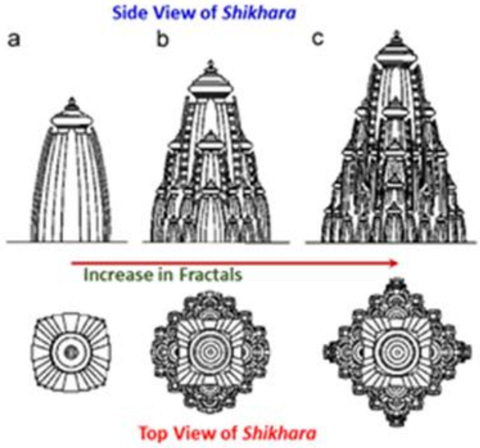

Figure 3: *Fractal architecture of the shikhara. (Source: Trivedi K. Hindu temples: models of a fractal universe [17])*

The image above was created using comparative elevations and plans of (a) the Shikhara of '*Adinatha*' temple (900 AD), (b) the Shikhara of '*Paraswanatha*' temple (950 AD), and (c) the Shikhara of '*Kandariya Mahadev*' temple (1050 AD) [17]. With an escalation in geometric complexity, the count of self-similar designs concurrently rises, implicitly reflecting the presence of fractal geometry.

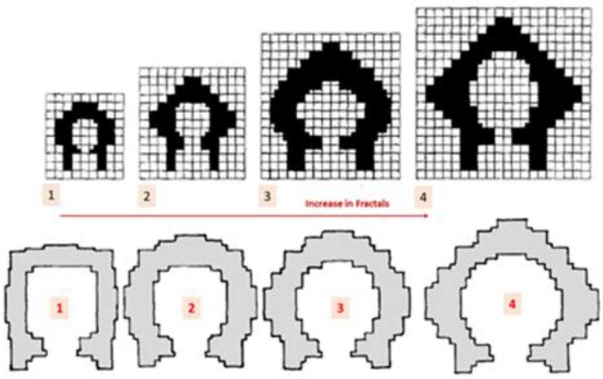

Figure 4: *Development of Garbh Griha in fractal sequence. (Source: Trivedi K. Hindu temples: models of a fractal universe [17])*

The increasing intricacy of elements on both the interior and exterior walls of diverse garbhagrihas is depicted in Figure 4. The inner wall showcases features such as (*1) Bhadra, (2) Subhadra, and (3) Pratibhadra*, while the exterior walls exhibit elements like *(1) Arya, (2) Hastangula, (3) Bhagava, and (4) Samadala.*

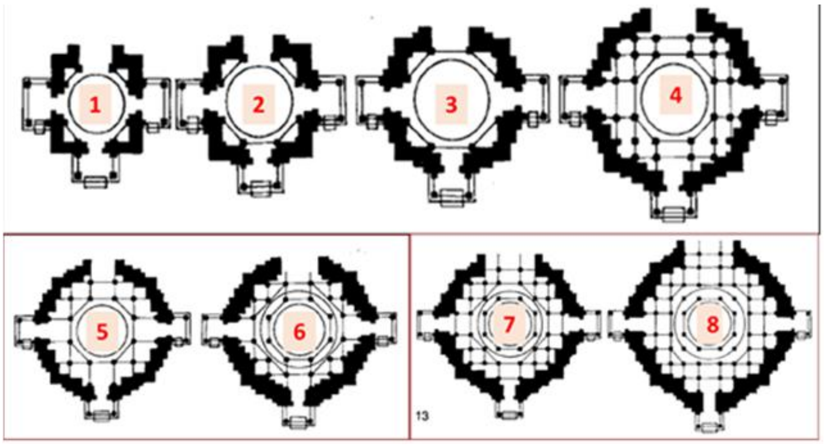

Figure 5: *Mandapa's fractal geometry in ascending order of fractal repetition. (Source: Trivedi K.. Hindu temples: models of a fractal universe [17])*

Figure 5 illustrates the plans of eight kinds of *Mandapas*, as outlined in *Shilpa* texts: *1. Vardharnan; 2. Swastika; 3. Garuda; 4. Suranandan; 5. Sarvatobhadra; 6. Kailash; 7. Indranila; 8. Ratnasambhava*. The external and internal wall geometry and elevation change, becoming increasingly creative and complicated in geometry from stage 1 to stage 8 of the mandapa geometry [18]. In some states, the design preserves symmetry concerning the x (horizontal) and y (vertical) axes.

Fractal architecture in temple design is a captivating exploration of fractal geometry principles, introducing intricate and self-repeating patterns into the very fabric of temple structures. This design concept, extending beyond mere aesthetics, weaves a tapestry of symbolic meaning into various facets of temple architecture. Exhibiting self-similarity, where patterns repeat at different scales within the structure, fractal architecture is discernible in the replication of specific design elements or motifs throughout the entire temple. The incorporation of intricate details at varying levels of magnification, facilitated by fractal geometry, manifests in temples adorned with highly detailed carvings, patterns, and reliefs, creating visually rich environments [19]. Geometric patterns, such as fractal curves, recursive structures, and shapes, form the foundation of this architectural approach, visible in the layout, pillars, and ornamentation of temples. Mandala designs, rooted in geometric principles and characterized by radial symmetry, represent a form of fractal architecture prevalent in temples, symbolizing the universe and embodying repetitive patterns.

Beyond aesthetic allure, the use of fractal geometry carries symbolic significance, portraying cosmic order, interconnectedness, and spiritual concepts of infinity and eternity. Embracing mathematical precision, fractal architecture demands meticulous planning, often employing algorithms to ensure a harmonious and balanced temple structure [20]. Associated with sacred geometry, fractal architecture aligns certain shapes like circles, squares, and triangles in a repeated fractal manner, imbuing spiritual significance. The result is visual harmony, where the repetition of patterns and shapes contributes to a sense of order and coherence, enhancing the overall aesthetic appeal [20]. This aesthetic complexity invites contemplation, encouraging worshippers and visitors to delve into the depths of architectural details with a sense of wonder. Culturally varied, fractal architecture in temples can take different forms across diverse cultures and historical periods, ranging from intricate complexity to simpler geometric patterns, each laden with symbolic meanings [21]. In essence, fractal architecture in temple design unites mathematical precision, symbolic depth, and visual richness to transcend mere functionality, providing a profound and aesthetically pleasing experience for all who enter.

8. Physical human form and Temple Geometry

Conferring to ancient sacred scripture or agamas, the temple is considered a body. Therefore, the construction of a temple must adhere to specific rules based on *Tantra, Agama*, and *Shilpa Śastra*. The '*Kśetra'* (temple area) represents our '*sthūla śarīra'* (gross body), the deity symbolizes the '*sūkshma śarīra'* (subtle body), and its '*prāña*' represents our '*kāraṇa śarīra'* (causal body). The '*prāña'* of the deity is considered analogous to ours. The temple structure, from feet to head, is comprised of six '*ćakras*' (Figure 6). Each part of the temple, such as *Garbhagriham*, *Dhwajasthambham*, etc., holds significance in Tantra *Śastra*.

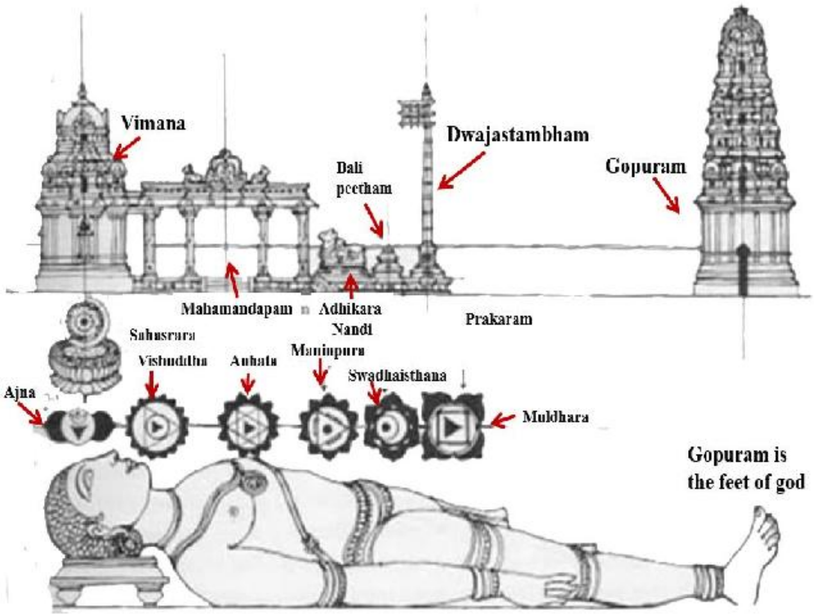

Figure 6: *Self-similarity is expressed in both the human body and temple geometry..(Source: Sthapati G.Thirugnnanam[22])*

9. Vinyasasutra (Layout & Orientation of Temple Complexes)

Hindu temple architecture is symmetrical and self-repeating, with its foundations in mythology, cardinality, and mathematics. The Vastupurusamandala principles are followed in the layout of the Manduka Hindu Temple floor plan, which is based on an 8x8 (64) grid. This 64-grid pattern stands as the most sacred and widely used template for Hindu temples. At its center, marked by a vibrant saffron hue, the intersection of diagonals symbolizes the Purusha in Hindu philosophy.

In a Hindu temple, the axis is determined by the four cardinal directions, forming a perfect square within the available space. This square is considered divine, symbolizing perfection, knowledge, and human thought. Surrounding the square is the circular mandala, representing earthly and human elements observed in everyday life. The relationship between the square and circle is symbiotic. The square undergoes division into grids, as depicted in Figure 7, commonly resulting in an 8x8 or 64-grid configuration within expansive temples. For ceremonial temple superstructures, the prevalence of an 81-square grid is notable. These individual squares, referred to as 'padas,' trace their origins back to the Vedic practices surrounding the fire altar, '*Agni'*. The configuration along basic directions serves as an extension of *Vedic* rituals, with Hindu temple manuals intricately detailing design plans that encompass square counts ranging from 1 to 1024. The most basic plan, featuring a single pada, functions as a seat for meditation, yoga, or conducting Vedic fire rituals. The design incorporating 4 padas boasts a symbolic vital core, fostering a meditative ambiance. In the 9 pada configuration, a sacred-surrounded center emerges, serving as the template for the smallest temple. While older temples may employ the 9 through 49 pada series, the 64-grid structure holds unparalleled sanctity in Hindu temple architecture, referred to as Manduka, Bhekapada, or Ajira [23]. Respectively pada is conceptually linked to a representative element or deity, with the central squares of the 64-grid specifically dedicated to the Brahman, known as Brahma padas. Ancient temple plans, like that of Tanjavur, (figure-8) were meticulously divided into architectural elements to fulfill these mathematical and symbolic calculations.

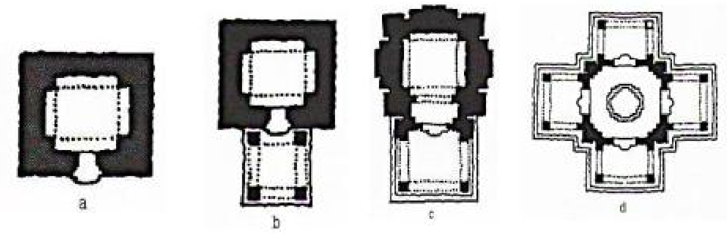

Figure 7: *Distinctive Temple Plan (a)Shrine without porch (b)Shrine with front porch (c)Shrine with front Antarala and porch (d)Sarvatobhadra - shrine with entrances on all four sides (Source: Hardy, Adam. The Temple Architecture of India [24])*

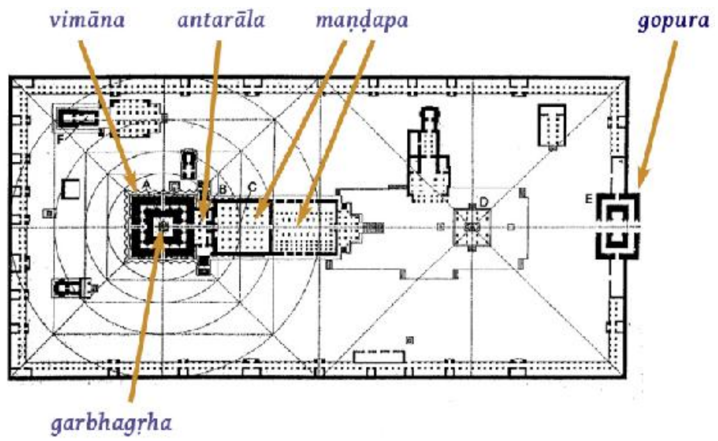

Figure 8: *Plan of Typical south indian Temple : Tanjavur (Source: Velmurugan C. and Kalaivanan R., Existence of the golden ratio in Tanjavur Brihadeeshwarar temple [25])*

10. The Technological Advancements in the Construction of Ancient Hindu Temples

According to the references, the temple's construction materials comprised stone slabs, metal plates, palm fronds, and timber parts. Dravidian and Nagara temple construction techniques were substantially similar, culminating in temple construction [26]. Minor variances arose as a result of factors such as the variety of construction materials, climate considerations, and the availability of manual labor during the construction process.

The building of the temples began with the gathering of a knowledgeable group under the direction of the chief architect, whose titles differed according to the location (sompuras in the western region, mahapatras in the eastern region, and Sthpatis in the southern region). The building team was divided into four different classes:

i. ***Sthapati:*** The chief architect, well-versed in traditional knowledge, mathematics, and *Shilpa shastras*.

ii. ***Sutragrahin:*** Responsible for executing tasks allocated by the "*Sthapati*".

iii. ***Taksaka:*** extensively involved in the precise shaping and engraving of stones.

iv. ***Vardhakin:*** The stonemason responsible for assembling all the individual components.

The sequence of temple construction is explained below;

1. **Planning the Temple:**
    - The construction of a temple, an extensive and lengthy process lasting years, commenced with meticulous planning.
    - The initial phase involved the selection and inspection of the site, determining the orientation and layout, and choosing materials. This process utilized the Indian Circle Method and an instrument known as "shanku yantra."
    - The orientation of the temple was significantly influenced by the nature of the main deity.
    - The chosen stone for construction had to exhibit specific qualities, including even color, hardness, and a pleasing tactile feel.
2. **Carving the Temple Parts:**
    - The subsequent phase focused on the intricate carving of different temple components. The takshaka guided sculptors and shilpis in carving according to specified drawings.
    - Stone cutting and carving adhered to predetermined shapes, and rough joinery was established during the cutting process.
    - Locally crafted tools such as hammers and chisels were regularly sharpened for use.
    - Sketching was executed using charcoal or sharpened bamboo, and the polishing process involved the use of stone bars.
3. **Assembling the Temple:**
    - The final stage encompassed the assembly of temple parts, marking the actual construction phase.
    - Mortise and tenon joints, a key joinery system involving a peg secure between two mortises in diverse stones, were prominently used. This method prevented movement due to lateral forces and was particularly employed between two courses of masonry (Figure 9). Lap joints were also utilized during assembly.

Figure 9: *Stone joined by iron pegs fixed as "X" joint. (Source: Parmar S. P., Insights of Modhera Sun Temple [27])*

- **Stone Wall Thickness:** The typical thickness of stones employed for constructing walls ranged between 800 mm to 1200 mm.
- **Column Structure:** The five integral pieces of a column were two segments that made up the base of the column, one segment that made up the shaft of the column, and two portions that made up the capital.
- **Monolithic Construction:** Both columns and beams were constructed as monolithic structures, ensuring a seamless and cohesive architectural integrity.

Hindu temples were established across a myriad of locations, each characterized by its distinct geography, topography, and meteorological conditions. As a result of this diversity, several building styles and materials were incorporated. Here are some instances of these many temple locations:

Temples in Varied Locations:

- *Mountain Temples:* Notable examples include Mansa Devi and Vaishno Devi.
- *Cave Temples:* Examples encompass Chandrabhaga and the Chalukya Ellora Caves.
- *Step Well Temples:* Prominent instances are *Mata Bhavani* stepwell and *Khodiyar Mata* stepwell, both situated in Ahmedabad, Gujarat.
- *Temples inside forests:* Locations like "*Kasaun*" and "*Kusama*" are representative of temples in forested areas.
- *River Bank and Seashore Temples:* Iconic temples situated along riverbanks and seashores include Jagannath Puri, Somnath, Kashi, Prayag (Allahabad), Hardwar, and Rameswaram, among others.

11. Art and Cultural representation in Temples

Art in Ancient Hindu Temples:

- *Diverse Art Forms:* Ancient Hindu temples boast a rich array of artistic expressions, encompassing paintings, sculptures, symbolic icons, engravings, and a well-thought-out spatial layout that integrates mathematical ideologies with the Hindu conceptualization of time and cardinal points.
- *Categorization of Idols and Images:* According to earliest Sanskrit scripts, idols and images are classified in various forms. One method involves the dimensionality of completion:

- **Chitra:** Referring to fully formed, three-dimensional images.
- **Chitrardha:** Describing pictures inscribed in partial relief.
- **Chitrabhasa:** Representing 2D pictures, such as portraits on walls and fabric.

12. Discussion

Temple architecture serves as a testament to the profound advancements achieved in the realm of ancient Indian building sciences. This paper intricately explores a spectrum of facets including styles, design geometry, philosophical underpinnings, construction technology, and the intriguing concept of self-similarity between the human body and temple elements [28]. The geometric intricacies of Indian temples, including the extent of work and the area they encompass, are contingent upon multifarious factors such as location, budget constraints, and the availability of specific building stones for construction. Across temporal and geographical dimensions, the geometry of temples undergoes dynamic transformations, adapting to the available materials and evolving design paradigms. The prevalent use of fractal architecture transcends various styles and regions of temple construction, persisting as a dominant practice even in contemporary times. The meticulous stone artwork adorning every facet of the temples appears to be meticulously crafted with the purpose of preserving and transmitting information. The shikhara's fractal geometry imparts an ambient aesthetic, achieving an exquisite equilibrium between mass and symmetry. Vertical offsets, increasing in a zigzag fashion with each side recess, contribute to a discernible vertical rhythm, while horizontal abutments and carvings enhance the structural stability of the temple The temple's geometric configuration is not merely an architectural feat; rather, it symbolically mirrors the human body, aligning with the sequential awakening of the seven chakras of Kundalini Shakti from feet to head. The thoughtful design, not only aesthetically pleasing but also resilient, was orchestrated to endure moderate seismic activities, reinforcing the temples as not just structures but profound symbolic representations of the human spiritual journey.

13. Concluding Remarks

- Temple architecture signifies profound advancements in ancient Indian construction technology.
- The paper explores elegances, geometrical design and styles, philosophical underpinnings, construction technology, and the concept of self-similarity with the human body.
- Geometric intricacies depend on factors like location of site, budget, and available building stones.
- Temple geometry evolves across time and geography, adapting to materials and design changes.
- Fractal architecture is a prevailing practice in contemporary temple construction.
- Stone artwork is meticulously crafted for the preservation and transmission of information.
- The *shikhara's* fractal geometry achieves an aesthetic balance between mass and symmetry.
- Vertical offsets in a zigzag fashion and horizontal abutments enhance structural stability.
- The temple's geometric configuration symbolically mirrors the human body and the awakening of chakras.

- The thoughtful design is both aesthetically pleasing and resilient, crafted to endure seismic activities, representing a profound spiritual journey.

References

1. Acharya, V. A. "*Indian Temple Architecture: form and Spaces*." Research Paper, Department of Architecture & Planning, I. I. T. Roorkee, (1991).
2. Christopher A, "*Building and Seismic Design Configuration, Pelham Books Ltd. F154*." Mac Graw Hill Inc. (1981).
3. Acharya P. K., "*An Encyclopedia of Hindu Architecture*" London. Q.U.P., (1946).
4. Barker, L. M. "*Pears Cyclopaedia*", London: Pelham Books Ltd. (1969).
5. Dagens, B. "*Mayamata: An Indian treatise on Housing architecture and iconography*". Motilal Banarsidass, (1985).
6. Fletcher S. B. and Cruickshank D. "*The History of Architecture.*" New Delhi: CBS Publishers and distributors, ISBN 075-06-2267-9, (1992).
7. Grover S., "*The Architecture of India: Buddhist and Hindu.*" Ghaziabad: Vikas Publishing House Pvt. Ltd., (1988).
8. Rian, I. M., Park, J. H., Ahn, H. U., and Chang, D. "*Fractal geometry as the synthesis of Hindu cosmology in Kandariya Mahadev temple*." Khajuraho. Building and Environment, 42(12), 4093-4107, (2007).
9. Kak, S. "*Space and cosmology in Hindu temples.*" Vaastu Kaushal: International Symposium on Science and Technology in Ancient Indian Monuments. New Delhi. November 16-17, (2002).
10. Kumar, N. "*The Hindu temple—where man becomes God*." The cultured traveler, vol. 7, (2005).
11. Dhaky, M. A. "*The Indian temple forms in Karṇāṭa inscriptions and architecture*." Abhinav Publications, (1977).
12. Meister, M. W. "*Geometry and measure in Indian temple plans: rectangular temples*." Artibus Asiae 44, no. 4, 266-296, (1983)
13. Bharne, V., and Krupali, K. "*Rediscovering the Hindu temple: the sacred architecture and urbanism of India*." Cambridge Scholars Publishing, (2014).
14. Prabhakar, S. "*The Vastu Vidya of Vishvakarma*." Studies in Indian Architecture, Asia, (1979).
15. Michell, G. "*The Hindu temple: An introduction to its meaning and forms*." University of Chicago Press, (1988).
16. Parashar R. et al., "*Fractal, architecture and sustainability*," Recent Research in Science and Technology 2014, 6(1): 93-96, ISSN: 2076-5061, (2014).
17. Trivedi, K. "Hindu temples: models of a fractal universe." The Visual Computer, 5(4), 243-258, (1989).
18. Vardia S. & Lourenco P. B. "*Building science of Indian temple architecture*". In the proceedings: The International conference on Rehabilitation and Restoration of Structures (ICI), IIT Madras, Chennai India. 12-16 February 2013. Pp.167-178, (2013).
19. Gupta S. P. and Vijayakumar S. Temples in India: Origin and Developmental Stages. D. K. Print wood (P) Ltd., New Delhi, (2010).
20. Parmar, S. P., & Mishra, D. P. Fractal Geometry in Water Conservation Structures: Step Wells and Tanks in India. Indian J. Hist. Sci, 55, 154675. (2020)
21. Dokras S., "*Hindu temple architecture of Bharat- Some Musings*." pp.1-30, (2009).
22. Sthapathi G. T. The Scientific Edifice of *Brihadeeswara* Temple Tanjore Tamilnadu. 2nd ed. Chennai: Dakshinaa Pub. House. (2003).

23. Gokhale V. A. “Architectural Heritage and Seismic design with reference to Indian Temple Architecture.” In Proceedings: 13th World conference on Earthquake Engineering, Vancouver, B. C., Canada August 1-6, (2004).
24. Hardy, A. The temple architecture of India. Wiley Academy, (2007).
25. Velmurugan, C., and Kalaivanan R. "Existence of the golden ratio in Tanjavur *Brihadeeshwarar* temple." Open Journal of Mathematical Sciences 4, no. 1, 211-219, (2020).
26. Sala, N. “*Fractal Geometry and Self-Similarity in Architecture: An Overview across the Centuries*.” ISAMA, pp. 235-244. (2003)
27. Parmar, S. P. “Insights of Modhera Sun Temple: Architectural Design and Its Site Significance.” Journal of Interior Designing and Regional Planning (e-ISSN: 2581-9984), 36-45, (2023).
28. Sarkar D. and Kulkarni S. “*Role of fractal geometry in Indian Hindu temple architecture*.” IJERT, ISSN: 2278-0181, Vol.4. Issue 05, pp.532-537, (2015).

CONTENTS

Published by
National Institute of Technical Teachers' Training and Research, Kolkata
(Ministry of Education, Government of India)
Block-FC, Sector-III, Salt Lake City, Kolkata-700106